Chem Soc Rev

REVIEW ARTICLE

View Article Online
View Journal | View Issue

Cite this: *Chem. Soc. Rev.*, 2015, 44, 7406

Phosphorus promotion and poisoning in zeolite-based materials: synthesis, characterisation and catalysis

Hendrik E. van der Bij and Bert M. Weckhuysen*

Phosphorus and microporous aluminosilicates, better known as zeolites, have a unique but poorly understood relationship. For example, phosphatation of the industrially important zeolite H-ZSM-5 is a well-known, relatively inexpensive and seemingly straightforward post-synthetic modification applied by the chemical industry not only to alter its hydrothermal stability and acidity, but also to increase its selectivity towards light olefins in hydrocarbon catalysis. On the other hand, phosphorus poisoning of zeolite-based catalysts, which are used for removing nitrogen oxides from exhaust fuels, poses a problem for their use in diesel engine catalysts. Despite the wide impact of phosphorus–zeolite chemistry, the exact physicochemical processes that take place require a more profound understanding. This review article provides the reader with a comprehensive and state-of-the-art overview of the academic literature, from the first reports in the late 1970s until the most recent studies. In the first part an in-depth analysis is undertaken, which will reveal universal physicochemical and structural effects of phosphorus–zeolite chemistry on the framework structure, accessibility, and strength of acid sites. The second part discusses the hydrothermal stability of zeolites and clarifies the promotional role that phosphorus plays. The third part of the review paper links the structural and physicochemical effects of phosphorus on zeolite materials with their catalytic performance in a variety of catalytic processes, including alkylation of aromatics, catalytic cracking, methanol-to-hydrocarbon processing, dehydration of bioalcohol, and ammonia selective catalytic reduction (SCR) of NO_x. Based on these insights, we discuss potential applications and important directions for further research.

Received 4th February 2015

DOI: 10.1039/c5cs00109a

www.rsc.org/chemsocrev

Inorganic Chemistry and Catalysis, Debye Institute for Nanomaterials Science, Faculty of Science, Utrecht University, Universiteitsweg 99, 3584 CG, Utrecht, The Netherlands. E-mail: b.m.weckhuysen@uu.nl; Fax: +31-30-251-1027

Hendrik E. van der Bij

Hendrik van der Bij received his PhD from the Inorganic Chemistry and Catalysis group of Utrecht University (The Netherlands) in 2014. His PhD research, under the supervision of Prof. Bert Weckhuysen, focused on the use of spectroscopy to study zeolite post-modifications. He currently works as a scientist at Albemarle Catalysts in Amsterdam, The Netherlands.

Bert M. Weckhuysen

Bert Weckhuysen received his master's degree in chemical and agricultural engineering from Leuven University (Belgium) in 1991. After obtaining his PhD from Leuven University in 1995 under the supervision of Prof. Robert Schoonheydt, he has worked as a postdoc with Prof. Israel Wachs at Lehigh University (USA) and with Prof. Jack Lunsford at Texas A&M University (USA). Weckhuysen has been since 2000 a full professor of inorganic chemistry and catalysis at Utrecht University (The Netherlands). His research interests are in the development of spectroscopy and microscopy techniques for elucidating the working and deactivation principles of catalytic solids, often applied under true reaction conditions.

1. Introduction

Biomass conversion, cracking of crude oil, automotive catalysis and gas-to-liquid technology[1–4] are just a few of the many chemical processes where zeolites are used or have the potential to be used as catalysts. Made from the abundant elements silicon, aluminium and oxygen, they are relatively cheap and environmentally friendly materials. In the expected transitional period where the global economy will move from fossil-based to truly sustainable resources, zeolites still have an important part to play. Therefore, it is essential to understand the chemistry of these fascinating shape-selective 'micron-scale molecule making factories' on a fundamental level, from the macroscale to the nanoscale. Insights into their morphology, accessibility, active sites, selectivity, stability and deactivation behaviour will allow us to further improve and extend their use as valuable catalyst materials.

An influential example of a zeolite material – and one very relevant for this review – is zeolite H-ZSM-5. Fig. 1 shows H-ZSM-5 on different dimensional scales. Single H-ZSM-5 crystals are often coffin- or parallelepiped-shaped and can have sizes ranging from 100 nm to 100 μm.[5–7] Inside the crystal we find a three-dimensional microporous channel system, as can be seen in Fig. 1b and c, which acts as transport channels for molecules. The channel system comprises straight and sinusoidal pores. Both pore types run parallel to the [010] and [100] crystallographic planes, respectively. As the two pore types are connected at regular intersections, molecules can diffuse in the [001] direction as well. The average pore size of these channels is around 5.5 × 5.5 Å.[8] At the positions where the microporous channels intersect, cavities form, which are 6.36 Å in diameter.[9] Consequently, molecules that exceed the dimensions of the channels are prevented from entering or exiting the zeolite. However, larger molecules can form in the cavities at the channel intersections. These shape-selective properties make H-ZSM-5 and zeolites in general effectively act as molecular sieves.

The channel system of H-ZSM-5 stems from a well-ordered MFI-type framework. All zeolite frameworks consist of silica and alumina tetrahedra, which are linked by shared oxygen atoms. The solid-acid character of zeolites arises from negatively charged AlO_4^- tetrahedra that are incorporated into the zeolite lattice. Each of these tetrahedra produces a net negative charge on the framework, which needs to be compensated by a counter-cation. If the counter-cations are protons, strong Brønsted acid sites are formed, as shown in Fig. 1e. If more aluminium is substituted in the framework, it leads to more acid sites. Therefore, the silicon to aluminium ratio in the framework is an important parameter for zeolites and is generally written as the Si/Al ratio. The combined shape selectivity and strong acidity of zeolites create the desired properties such as catalytic cracking of hydrocarbons.

Although the majority of zeolites are used as hydrocarbon cracking or isomerisation catalysts in oil-refining processes, zeolites are also used in many other catalytic processes, including alkylation of aromatics with oxygenates, conversion of (bio)alcohol to light olefins, dewaxing of hydrocarbons, aromatics and fuels, dehydrogenation of paraffins, and dehydration of (bio)alcohols, and in photocatalytic reactions.[10–26] It is therefore the case that zeolites are not just catalysts for present-day oil-refining purposes, but are also important catalysts for future green/clean hydrocarbon production processes.

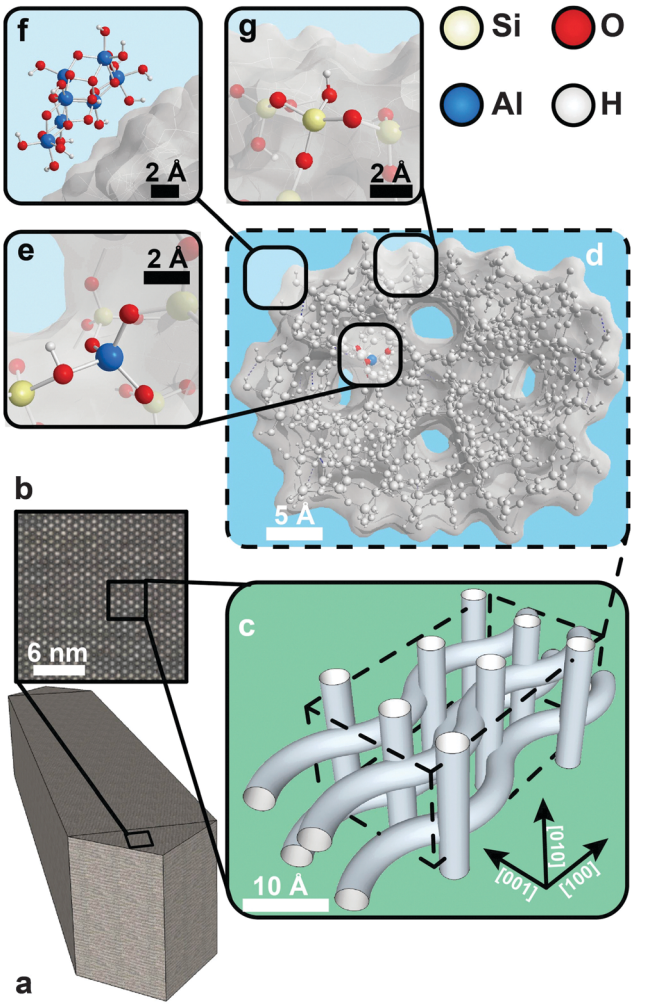

Fig. 1 Overview of zeolite H-ZSM-5 on different dimensional scales. (a) A micron-sized coffin-shaped H-ZSM-5 crystal. (b) Closer inspection of the [001][100] plane, revealing straight pores. (c) The three-dimensional channel system of H-ZSM-5 consists of intersecting straight and sinusoidal pores. (d) The channel system is derived from the MFI framework, which comprises linked silica and alumina tetrahedra. (e) A tetrahedrally coordinated framework aluminium (TFAl) atom produces a net negative charge on the framework. In H-ZSM-5 this negative charge is compensated by a proton, which generates a Brønsted acid site. The OH group in SiOHAl is generally referred to as a bridging hydroxyl group. (f) Dealumination leads to the formation of extra-framework aluminium, here shown as boehmite. (g) Terminal silicon and aluminium atoms, which are generally found on the external surface of a zeolite, form silanol and aluminol groups.

In the late 1970s, it was found that post-modification with a phosphorus precursor can change the acidic and shape-selective properties of zeolites.[10,27–30] The most notable phosphorus-containing precursor is H_3PO_4, which is added to a zeolite by wet impregnation. After this step, the zeolite is thermally treated in air/oxygen, a process better known as calcination, which decomposes phosphorus precursors into (poly)phosphates and phosphorus pentoxide. It has been found that phosphorus can act towards

zeolites either as a promoter, *e.g.*, in the fluid catalytic cracking (FCC) process and the methanol-to-hydrocarbons (MTH) reaction, or as a poison, as in ammonia selective catalytic reduction (NH_3-SCR) of exhaust gases, *i.e.*, NO_x.[27,31,32]

As a promoter, phosphorus is well known to improve the hydrothermal stability of zeolite H-ZSM-5.[33,34] At the same time, phosphorus interacts with the acid sites of zeolites, leading to a reduction in the number and strength of acid sites.[35] Furthermore, if phosphorus is located in the micropores of a zeolite, it can either favourably alter its shape-selective effects or block the micropores and reduce the overall accessibility of the zeolite material.[36] Although the presence of phosphorus can be beneficial, for example in the MTH reaction where it boosts selectivity towards light olefins and especially towards propylene,[31] it is deleterious for NH_3-SCR nitrogen oxide-removing applications.[37]

The promotional effects of phosphorus are well known to the refining industry, which follows from the numerous patents involving all major refining companies.[23,38–49] Not surprisingly, many academic groups have reported on the effects of phosphorus on zeolites. However, the exact nature of phosphorus–zeolite interaction has always been a point of discussion, which makes phosphorus–zeolite chemistry an important topic from a fundamental perspective as well. Many models of possible interactions have been proposed over the years and the main division of opinion regards the question of whether a permanent phosphorus–framework interaction exists or not.[34,50–56]

In the case of a permanent phosphorus–framework interaction, the most intuitive explanation would be the incorporation of phosphorus into the zeolitic framework. Examples of these suggestions are shown in Scheme 1a–d. These interactions can be subsequently categorized into (a–b) phosphorus bonded to the bridging oxygen group of Si–O–Al,[52,57] (c) Si–O–P bonds,[35] and (d) Al–O–P bonds.[55,58] Other possible phosphorus–framework interactions have been suggested as being reversible, as shown in Scheme 1e and f.[34,50,59] Examples of suggestions for reversible interactions are (e) intramolecular bonds[59] or (f) protonation of phosphoric acid by bridging hydroxyl groups in the zeolite.[34] It has also been proposed that (g) phosphorus does not interact at all with the zeolite framework and only interacts with extra-framework aluminium.[56]

We believe that the topic of phosphorus–zeolite chemistry will become increasingly important for three reasons: (i) hydrothermal stabilisation of zeolites is essential for the industrial application of zeolites as catalysts to produce hydrocarbons. Especially during regeneration after deactivation of coke, conversion of (bio)alcohol and dehydration, the presence and formation of water combined with high temperatures lead to permanent deactivation of zeolite catalysts.[60–62] (ii) There is an ever-increasing demand for propylene and its selective production using phosphated zeolites is a serious candidate for selective large-scale production.[31,63,64] (iii) The relatively high phosphorus content in biofuel poses a challenge for zeolites as NH_3-SCR catalysts.[65]

Elucidation of the nature of phosphorus–zeolite chemistry is expected to reveal the reasons behind hydrothermal stabilisation, alteration of the acid site and changes in catalytic performance. This review article provides the reader with a thorough analysis of the academic literature on phosphorus–zeolite chemistry, which has, to the best of our knowledge, never been the subject of a review paper. The goal of this review article is to find structural and physicochemical trends in phosphorus-modified zeolites. Subsequently, we aim to link these structural properties to catalytic poisoning and promotional effects found in catalysis. The review article ends with an outlook to future research directions.

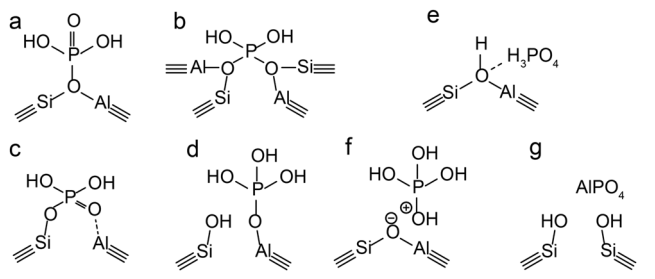

Scheme 1 Suggestions from the literature for phosphorus–framework interactions. (a–c and f) Are most cited. (a) Kaeding *et al.*,[52] (b) Xue *et al.*,[57] (c) Lercher *et al.*,[35] (d) Zhuang *et al.*,[58] (e) Abubakar *et al.*,[59] (f) Blasco *et al.*,[34] and (g) Caro *et al.*[56]

2. Methods of phosphorus introduction

When considering the vast literature on zeolites modified by phosphorus, it is clear that incipient wetness impregnation (IWI) or wet impregnation (WI) is the most practised method of phosphatation.[31,33,34,50,51,53,57–60,63,64,66–85]

The precursor of choice is phosphoric acid.[10,31,33,34,50,51,53,55,58,63,64,66–68,70,71,73,75,77,78,81–87] Less acidic precursors such as $NH_4H_2PO_4$[34,36,88,89] and $(NH_4)_2HPO_4$[57,60,69,74,76,79,80,86] are used as well. After impregnation, the materials obtained are first dried at temperatures ranging from 70 °C to 120 °C, sometimes at reduced pressures. Afterwards, samples are calcined at elevated temperatures ranging from 450 °C to 650 °C for durations ranging from 1 h to 6 h.

Another preparation method is quite similar to impregnation, with the difference that the sample is mixed under reflux conditions with an aqueous solution of H_3PO_4, where the concentration of H_3PO_4 corresponds to the desired phosphorus content. Water is removed by evaporation at reduced pressure. Subsequently, the samples are dried and calcined.[35,54,56,86,87,90–92]

Besides phosphoric acid and ammonium phosphates, different precursors are used as well. Especially popular in the 1980s was the use of trimethylphosphite (TMPT). This precursor was dissolved in *n*-octane and mixed with a zeolite slurry. The mixture was stirred under reflux conditions, then filtered, washed with, *e.g.*, *n*-pentane and dried at 120 °C. Subsequently, the sample was calcined at elevated temperatures.[29,52,54,90,93,94] Gas-phase deposition is also a technique used to transfer a phosphorus precursor into H-ZSM-5 zeolite. Precursors reported with this technique are trimethylphosphite (TMPT),[78,94,95] triphenylphosphine (TPP),[96,97] trimethylphosphine (TMP)[54,59,90–92] and phosphorus pentachloride (PCl_5).[98] The zeolite was contacted with the vapour phase of

these precursors at elevated temperatures ranging from 360 °C to 600 °C. In the case of TMP a cycle was repeated twice.

Different precursors used in combination with impregnation methods are diphenylphosphinous (DPP) acid, TPP and phosphorus trichloride (PCl_3), dissolved in methylene chloride, carbon tetrachloride and benzene, respectively.[17] However, it is important to understand that all these methods are followed by a post-calcination process, which converts the phosphorus precursors into phosphates.

Finally, attempts have been made to incorporate phosphorus into the MFI framework by synthesizing ZSM-5 with a phosphorus precursor in the reaction gel.[99,100] Gao *et al.* used a phosphatation method which was named the hydrothermal dispersion method. Here, H-ZSM-5 is mixed with $(NH_4)_2HPO_4$ and reacted at 140 °C and 0.3 MPa for 2 h.[101,102]

Although there are many different ways to introduce phosphorus, it can be seen in the following sections that the overall physicochemical effects on the zeolite structure are very similar. Nevertheless, significant differences that arise due to the method of phosphorus introduction used will be highlighted when applicable.

3. Physicochemical changes

3.1 Physical and chemical phosphorus–framework interactions

In the following section we will describe three distinct phases that can be found in phosphated zeolites, which consist of (i) separate phosphate and zeolite phases (ii) a phosphate–zeolite interface phase and (iii) separate aluminium-phosphate and zeolite phases. The formation of these phases depends strongly on the pre- and post-treatment of the zeolite during phosphorus introduction. However, it is important to understand that these phases often exist simultaneously in phosphated zeolites.

3.1.1 Separate phosphate and zeolite phases. As was mentioned in the previous section, the method of choice for phosphatation is the introduction of phosphoric acid to a zeolite by means of wet impregnation. Several characterization methods have indicated that this method leads to a higher concentration of phosphorus species on the zeolite surface compared to phosphorus in the zeolite bulk.[29,37,51,86,87,96] Most of these species are monomeric phosphates and di- or polyphosphates.[56] Generally, smaller phosphate chains are found before calcination of the zeolite, whereas larger condensed polyphosphate species and phosphorus pentoxide form after heat treatment due to dehydration.[59,86] Rehydration hydrolyses phosphorus pentoxide species to give mono-, di- and small polyphosphate chains.[56,59] Lischke *et al.* showed that smaller phosphates could easily be removed by elution with hot water. However, the condensed polyphosphates that form after thermal treatment prove more difficult to remove by washing with hot water.[36,50,55,67,85,86] The majority of these phosphorus species exhibit no interaction with the zeolite phase and therefore the phosphate and zeolite phases can be considered separate. Nevertheless, the phosphate species have an influence on the accessibility of the zeolite, as will be discussed in Section 3.2.

3.1.2 Phosphorus–aluminium attraction: reversible interfaces. As phosphorus is mainly found on the zeolite surface as a separate phosphate phase, only a relatively small amount of phosphorus enters the pores of the zeolite. However, with an increase in phosphorus loading more phosphorus moves into the channel system.[33,34,53,56,58,71,77,81,84,86,87] There, phosphate species can form reversible and irreversible interfaces with framework aluminium. It has been shown that phosphoric acid can coordinate with tetrahedrally coordinated zeolite framework aluminium (TFAl), which induces octahedral coordination in aluminium.[69] This change from fourfold to six fold coordination is fully reversible, as washing with hot water removes phosphorus and reconverts six-coordinated aluminium into classic TFAl atoms.[50,86] An increase in phosphorus loading leads to increased occurrence of these interactions as more phosphorus enters the zeolite pores.[67] After thermal treatment of phosphated zeolite, these interactions remain reversible.[50,67,85,86] Suggestions for the nature of these reversible interactions include TFAl atoms that are physically coordinated by phosphate species[86] or ionic bonding[34,67] and a postulated structure is shown in Scheme 2a.

Besides a change in the coordination of aluminium, the presence of phosphoric acid can distort the electronic environment of TFAl atoms, which has been suggested to arise from hydrogen bonding between hydrogen atoms in H_3PO_4 and framework oxygen and/or Brønsted acid sites and phosphate oxygen groups.[59,86,103] Also, this type of interaction has been found to be fully reversible.[86]

Both types of interaction lead to an observable decrease in TFAl species and a reduction in Brønsted acid sites, as we will discuss in the following sections.[30,50,67,86] Permanent damage to the framework before thermal treatment of phosphated zeolites has not been reported for the MFI topology. However, as we will see in Section 3.1.4, other topologies appear to suffer damage to the framework after phosphorus introduction.[30]

3.1.3 Phosphorus–aluminium attraction: permanent interfaces and SAPO-fication. During thermal treatment, high temperatures and the presence of H_2O in the atmosphere will lead to the hydrolysis of Si–O–Al bonds (Fig. 2a and b).[106] In the presence of phosphorus even more Si–O–Al bonds are hydrolysed.[56,58,59,82,87] This effect can be observed in Fig. 2, where the decrease in the percentage of Si–O–Al bonds is plotted against the P/Al ratios in phosphated and thermally treated zeolites.

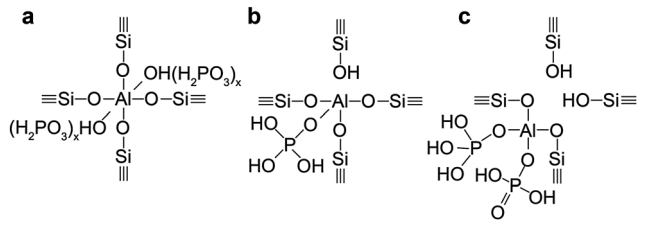

Scheme 2 Suggestions for different phosphorus–zeolite interface phases found in phosphated and thermally treated H-ZSM-5. (a) TFAl forced into six fold coordination by physically bonded phosphate species (b) local SAPO interface (c) local SAPO interface with aluminium connected to two phosphates.[55,58,71,86]

The figure indicates a trend that depends on the P/Al ratio, which suggests phosphorus species actively promote the hydrolysis of Si–O–Al bonds during thermal treatment. With high phosphorus loadings above 2.5 wt%, internal silanol groups at defect sites have been reported to form.[53,64,94,107] The exception is the work of Blasco *et al.*, where no dealumination is observed. In the relevant work, post-calcination of the sample was mild (500 °C, 1 h), which could have been insufficient for cleaving Si–O–Al bonds. The decrease in the percentage of Si–O–Al bonds is accompanied by a decrease in classic TFAl atoms.[33,34,37,50,53,55–59,67,69,71,77,78,81,82,84–87,92,98,108–111]

Due to the decrease in the percentage of Si–O–Al bonds, the crystallinity of zeolites may be reduced to a small extent after the introduction of phosphorus and subsequent thermal treatment, but the framework structure is maintained and no additional crystalline phases have been reported.[30,53,58,63,64,71,73,76,77,81–84,101,110] A loss of crystallinity was found for samples treated with acidic and non-acidic precursors and with the use of impregnation solutions of different acidities, excluding acid leaching as the source of the loss of crystallinity.

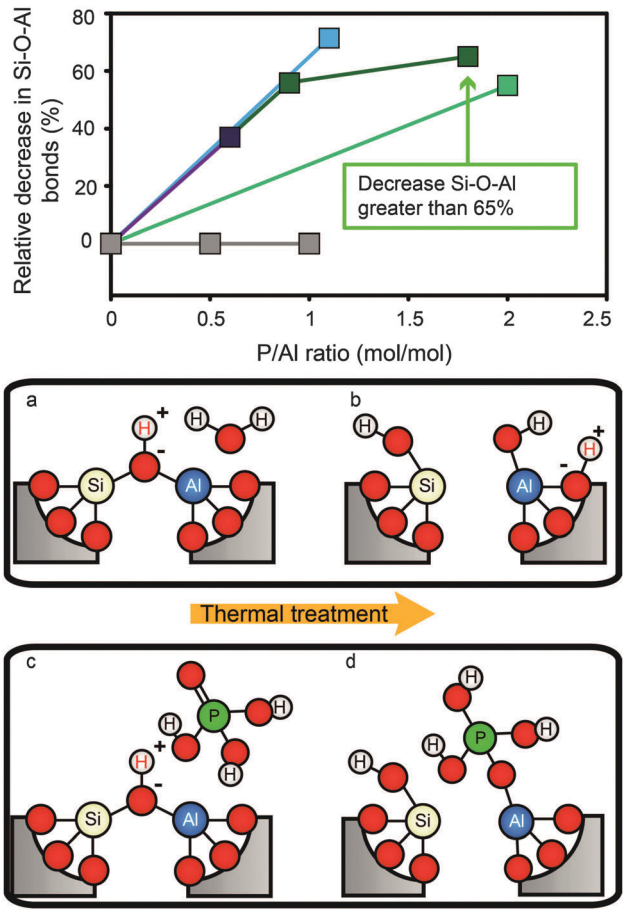

Fig. 2 Decrease in Si–O–Al bonds *vs.* P/Al ratio after phosphatation. Values are calculated from reported Si/Al ratios obtained by ^{29}Si MAS NMR. ■ = Caro *et al.*[56] ■ = Zhuang *et al.*[58] ■ = Abubakar *et al.*[59] ■ = Blasco *et al.*[34] ■ = Li *et al.*[82] The decrease in TFAl for P/Al ratio 1.8 corresponds to a reported Si/Al ratio that is greater than 200, so the actual percentage is higher. (a–d) Postulated mechanism of "SAPO-fication" by hydrolysis of Si–O–Al bonds during thermal treatment in the presence of H_2O and H_3PO_4.[55,58,60,67,86,104,105]

After thermal treatment of phosphated H-ZSM-5, H-ITQ-13, and H-MCM-22, a new type of aluminium is formed at the expense of classic TFAl atoms.[33,34,57,58,67,71,75,82,85–87,92,110,112] In other zeolite topologies these species are not observed.[30,37,108] This new type of aluminium can mostly be attributed to four-coordinated but also to five- and six-coordinated aluminium species that are still present at lattice positions in a highly distorted environment due to chemical and spatial interactions with phosphate species.[55,58,67,71,86] It is suggested that phosphate species bond with terminal Si–O–Al–OH groups of partially dislodged TFAl species that form during thermal treatment (Fig. 2b), which effectively leads to the formation of local silicoaluminophosphate (SAPO) interfaces (shown in Fig. 2c and d).[58,71,86] It is expected that the positively charged $[PO_4]^+$ unit at the SAPO interface balances the negative charge on the zeolite framework. ^{27}Al–^{31}P INEPT-HETCOR NMR experiments have confirmed that these species contain Al–O–P bonds.[55]

During this "SAPO-fication" process the zeolite material undergoes a gradual increase in this new SAPO interface phase with an increase in phosphorus loading.[34,53,67,71,82,92,107] However, a maximum amount of SAPO interfaces has been observed.[67,71,107] Local SAPO interfaces do not disappear after washing with hot water.[67,85,86] However, washing with NH_4F did remove the species.[34]

Importantly, Damodaran *et al.* have shown that local SAPO interfaces are not a single defined species, but consist of a variety of framework aluminium–phosphorus interactions, *e.g.* phosphate mono- and bidentate ligands on four-, five-, and six-coordinated aluminium atoms, of which a few are shown in Scheme 2b and c.[55,71] With higher phosphorus loadings the spectroscopic signatures of phosphorus in local SAPO interfaces become more like that of $AlPO_4$.[55,113] This indicates that more Si–O–Al bonds are broken and replaced by Al–O–P bonds with an increase in phosphorus content.[55,58,113] The aforementioned increase in Si–OH groups with an increase in P content agrees with this model.[53,64,94,107] Neither different pH values nor phosphorus precursors seem to have an influence on the appearance of local SAPO interfaces after thermal treatment.[34,78,86] The SAPO-fication model has also been proposed in environmental and soil science studies, where mesoporous silicates impregnated with aluminium are effective absorbers of phosphates from the environment, as phosphates are suggested to form Si–O–Al–O–P(HO)$_3$ monolayers.[114]

All the findings described in this section indicate an attraction between phosphorus and framework aluminium. Furthermore, there is a synergistic effect between the presence of phosphorus and subsequent heat treatment, as phosphorus actively promotes the dealumination of zeolites during thermal treatment, which indicates that the formation of Al–O–P bonds is energetically favoured.

Although in the last ten years more indirect evidence of framework-connected Si–O–Al–O–P(HO)$_3$–R species has been reported, the existence of SAPO interfaces has not yet been directly proved.[55,58,67,71,86,107] In order to clearly confirm bonding

between phosphorus and framework aluminum we suggest the addition of *J*-coupling ^{27}Al–^{29}Si correlation NMR spectroscopy[115] in combination with *J*-coupling ^{27}Al–^{31}P correlation NMR spectroscopy.[55]

3.1.4 Aluminium-phosphate formation. The attraction between phosphates and aluminium is even stronger when aluminium is present as extra-framework aluminium (EFAl) in zeolites. Phosphoric acid will readily react with any extra-framework aluminium species present in zeolites.[28,30,50,58,87,98,113,116] Several spectroscopic techniques have shown that EFAl species disappear when phosphorus is introduced to zeolites.[28,34,50,64,70,87,92,113] It has been established that extra-framework AlO(OH) species that were present before phosphatation will react with phosphorus and form an extra-framework amorphous $AlPO_4$ phase.[28,50,87,113,116] This amorphous $AlPO_4$ phase is heterogeneously distributed and mostly found on the external surface of zeolites, as shown in Fig. 3.[28,113] Thermal treatment leads to crystallisation of this phase as α-cristobalite/tridymite $AlPO_4$ islands.[28,30,87,113] It has not been observed that the $AlPO_4$ phase migrates during thermal crystallisation.[113]

In the case of the zeolites mordenite, ZSM-11, MCM-22 and zeolite Y, treatment with a phosphate precursor does not only lead to the reaction of phosphoric acid with extra-framework aluminium. Framework aluminium is leached from the lattice by phosphorus and amorphous $AlPO_4$ is formed.[30,82,98,108,112,113,116] The tendency of framework aluminium to be leached from the lattice by acid treatment depends on the topology of the zeolite.[117] In the case of USY, which has high aluminium content in its framework, extraction of framework aluminium leads to the collapse of the structure.[113] In the case of mordenite, almost all TFAl atoms are leached out of the framework, while the overall framework remains intact.[113] Although the effect of topology on the extraction of lattice aluminium by phosphorus would benefit from further systematic study, these findings exemplify the attraction between phosphorus and aluminium.

3.1.5 Phosphorus framework incorporation? In the previous sections we have seen that it is phosphorus–aluminium interaction that drives physicochemical changes in zeolites. However, especially in the early literature, it has been suggested that phosphorus is incorporated into the zeolite framework. This is understandable, as it would be the most intuitive explanation for the changes observed in zeolites upon phosphatation. However, in order for phosphorus to be incorporated into the framework, stable Si–O–P bonds need to be formed. In contrast, many theoretical works have shown that Si–O–P bonds are very unstable.[118–122] However, in one theoretical study it was suggested that the substitution of penta-coordinated phosphorus into the framework is possible at high temperatures.[109] However, experimentally, the work of Barrer *et al.* has shown that attempts to substitute phosphorus for silicon and aluminium in silicates and aluminosilicates only leads to the formation of $AlPO_4$ and silica.[123]

In a frequently cited study by Xue *et al.*, it was proposed that phosphorus is incorporated into vacant framework positions in dealuminated H-ZSM-5, for which convincing spectroscopic evidence was given (see Scheme 1b).[57] However, a detailed study on the formation of phosphosilicate glasses shows that the spectroscopic signatures Xue *et al.* attributed to Si–O–P species in fact stemmed from polyphosphate species that were trapped in a siloxane (or silica) framework and did not have any interaction with silicon species *via* a bond.[124] In this work, it was convincingly argued that P–OH and Si–OH groups rather self-condense than form cross-links.[124] The only Si–O–P bonds in phosphosilicate glasses that have been unequivocally assigned by means of *J*-coupling NMR spectroscopy have NMR resonances, which, to the best of our knowledge, have never been reported in the literature on phosphated zeolites.[125]

Therefore, due to the unstable character of Si–O–P bonds compared to the stable character of Al–O–P bonds and the lack of any experimental evidence,[126] it seems highly implausible that Si–O–P bonds easily form in phosphated zeolites and complete framework incorporation of phosphorus is thus very unlikely.

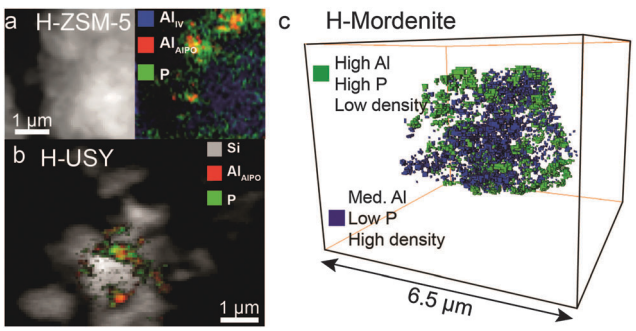

Fig. 3 X-ray absorption microscopy results show $AlPO_4$ 'islands' in phosphated (a) H-ZSM-5, (b) H-USY and (c) H-mordenite. Adapted from ref. 87 and 113.

3.2 Changes in porosity, accessibility and acidity induced by phosphorus

In the previous section we discussed what type of phases and interactions can be found in phosphated zeolites. The following section will discuss the effect of these phases and interactions on the porosity, accessibility and acidity of the zeolite.

3.2.1 Location and distribution of phosphorus. As we mentioned before, several characterization methods have shown that there is a higher concentration of phosphorus species on the zeolite surface compared to phosphorus in the zeolite bulk (Fig. 4a).[29,37,51,86,87,96] The method of phosphorus introduction seems to play an important role in the distribution of phosphorus. It has been reported that by using the hydrothermal dispersion method to introduce phosphorus, as mentioned in Section 2, more homogeneous distribution throughout the micropore channel system can be obtained, whereas impregnation leads to a high concentration of phosphorus species on the surface.[101,102]

Although most phosphate species present on the external surface have no interaction with the zeolite phase, it has been shown that the presence of phosphorus on the external surface of a zeolite is accompanied by a decrease or disappearance of surface hydroxyl groups after phosphatation.[54,56,69,72–74,86,87,92,94] In agreement with the presence of a phosphorus distribution gradient is the fact that at low loadings, below 2 wt% P, the

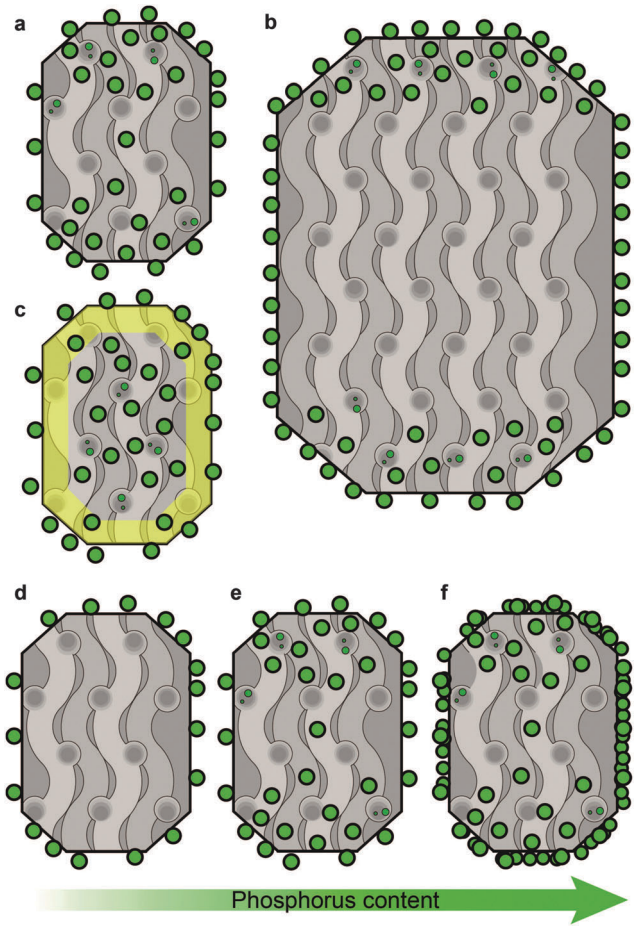

Fig. 4 Proposed schematic model of the location of phosphorus species depending on crystal size, aluminium distribution and increasing weight loadings of phosphorus. The model is based on XPS data from ref. 29, 51 and 96, ^{129}Xe NMR and ^{1}H NMR tracer desorption from ref. 56 and 69 and STXM studies.[86,87] (a) Typical distribution of phosphorus on H-ZSM-5. (b) Effect of crystal size. (c) Effect of aluminium distribution. Yellow indicates an aluminium-poor region. (d–f) Effect of increasing phosphorus loading. Due to diffusion limitations, the location of phosphorus is more dependent on the actual weight loading of P than on the P/Al ratio. Crystals are viewed along the [100][001] plane.

amount of surface hydroxyl groups decreases faster than that of those found in the bulk. Only when the surface is covered with surfactant do phosphorus species enter the zeolite bulk immediately at low loadings, as shown in Fig. 4d.[54,56,69,72–74,86,87,92,94] The latter results would indicate that phosphate species first form a phosphate–zeolite interface phase with external silanol and aluminol groups.

With an increase in crystal size, the ratio of $P_{Surface}/P_{Bulk}$ species increased (Fig. 4b).[51] This suggests that phosphorus species experience diffusion limitations. Interestingly, when the concentration of aluminium was higher in the zeolite bulk than on the external surface, the distribution of phosphorus was homogeneous (Fig. 4c).[29] This latter finding is in accordance with the previously described attraction between framework aluminium and phosphorus.

When phosphorus loadings are increased, phosphorus species tend to move further into the zeolite, as it was found that all aluminium species and corresponding acid sites are affected by the presence of phosphorus (Fig. 4e).[33,34,53,56,58,71,77,81,84,86,87] However, with progressively increasing phosphorus loadings the concentration of phosphorus surface species increases faster than that of those in the bulk and after phosphorus loadings exceed 5 wt% excess phosphorus is mostly deposited on the external surface.[35,37,53,55,56,69,78,81] Platelets of excess polyphosphates have been found to be present on the outer surface.[35] A schematic drawing of this effect is presented in Fig. 4f. Evidence for the aggregation of zeolite particles by phosphorus modification can be found in the literature as well and it has been suggested that phosphorus promotes the self-annealing of external Si–OH groups.[56,67,87]

The distribution gradient of phosphorus has recently been illustrated by our group in a spatially resolved manner using X-ray absorption microscopy and representative images are shown in Fig. 5. From the figure, it can also be observed that by introduction of phosphorus using wet impregnation heterogeneities in the phosphorus distribution between particles can be found.[86,87]

In summary, the weight loading of phosphorus, P/Al ratio, surface OH groups, aluminium distribution, crystal size and phosphorus introduction technique all play a role in the eventual distribution of phosphorus species.

3.2.2 Accessibility and porosity. As phosphorus is present on the external surface and in micropores, the phosphatation of zeolites leads to a decrease in micropore volume and surface area. As more phosphorus is able to penetrate the zeolite interior at higher weight loadings, this decrease gradually becomes more severe with an increase in phosphorus content.[30,31,33–35,53,57,64,67–69,71,73,74,76–79,81–85,87,89,102,107,110,113,127–129] Commonly, the decrease in micropore volume and surface area is attributed to dealumination, partial blockage of channels by phosphorus species and aggregation of zeolite particles. Chen *et al.* suggested that the presence of phosphorus changed diffusion characteristics by decreasing pore dimensions and openings, which led to longer diffusion pathways for reactants and products.[10,17,93] These results have been confirmed and Janardhan *et al.* reported that phosphorus forms monolayer islands throughout the MFI channel system.[36,69] Adsorption of the probe molecules cyclohexane and *n*-heptane indicated a strong decrease in accessibility for samples with more than 3 wt% loading of phosphorus species.[68]

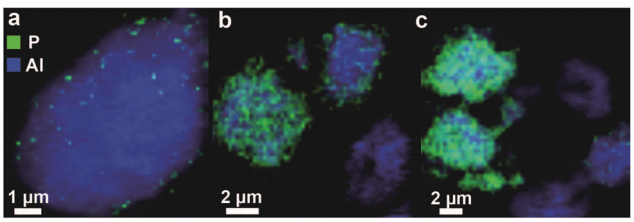

Fig. 5 X-ray absorption microscopy results, modified from ref. 86 and 87. Chemical maps of clusters of zeolite H-ZSM-5 (Si/Al = 11.5), modified by wet impregnation with a phosphate precursor followed by calcination (P/Al = 0.5), are constructed from aluminium K-edge spectra and phosphorus K-edge spectra stacks. Precursors used are (a and b) H_3PO_4 and (c) $(NH_4)_2HPO_4$. ■ = Al ■ = P, resolution is 60 × 60 nm.

When a phosphate precursor is used to introduce phosphorus, most of the phosphorus is present as ortho-, pyro-, and polyphosphates before thermal treatment.[67,86] As a proportion, up to the majority, of these soluble species can be removed by washing with hot water before thermal treatment, the external surface area and micropore volume of phosphated zeolites can be restored to 95% of those of the parent material.[53] However, washing a phosphated zeolite after thermal treatment leads only to a partial restoration of surface area and micropore volume.[36,53,85,89] One of the reasons for this situation is that after thermal treatment phosphorus species become condensed and occluded and have decreased solubility in water, whereas the other is the formation of a permanent phosphorus–zeolite interface phase, as discussed in Section 3.1.[67,86]

Nevertheless, it can be observed that most of the loss in micropore volume and surface area that is detectable by physisorption techniques is caused by the presence of water-soluble (poly)phosphate species. Seo *et al.* suggested that changes in micropore volume caused by (permanent) phosphorus–framework interactions were too small to detect by conventional physisorption methods, but could be distinguished by ^{129}Xe NMR spectroscopy.[69]

3.2.3 Acid site loss. The solid acid sites in zeolites are the active sites in zeolite catalysis. As discussed in the introduction, a perfect crystalline zeolite material has only three types of acid sites. The strongest acid sites are formed by the protons present in framework bridging hydroxyl groups, whereas the remaining acid sites are very weak and comprise surface terminal silanol and aluminol groups.[111] Thermal treatment, which is applied to convert the ammonium form of zeolites into H-zeolites, can lead to dealumination.[106]

With the breaking of Si–O–Al bonds, new acid sites can form. These are silanol groups that form at defect sites and extra-framework aluminium species.[111] Furthermore, framework aluminium species that are only partially connected to the framework can form Lewis or Brønsted acid sites.[86,130,131]

After modification of zeolites with phosphorus followed by thermal treatment there is a gradual decrease in bridging hydroxyl groups and silanol groups, with an increase in phosphorus content.[29,31,34–36,50,53,54,56–58,60,64,66–70,72,73,76–79,81–87,89,90,92,94–96,110,112,116,127–129] Within a single study, as can be seen in Fig. 6, the relative decrease in Brønsted acid sites correlates quite well with the P/Al ratio.[34] In the same study, it was established that all acid sites were accessible to molecules of probes and that the decrease in the number of acid sites can therefore most likely not be attributed to physical blocking of acid sites.

As all reported examples have been thermally treated after phosphatation, one obvious cause of the loss of Brønsted acid sites is dealumination induced by thermal treatment. The breaking of Si–O–Al bonds and formation of Al–OH groups have been observed after phosphatation and subsequent calcination.[56,58,59,82,84,86,94,132] Thermal treatment can contribute to at least 45% of the loss in strong acid sites.[86] Furthermore, as phosphorus promotes the hydrolysis of Si–O–Al bonds, a gradual decrease in acid sites with an increase in phosphorus

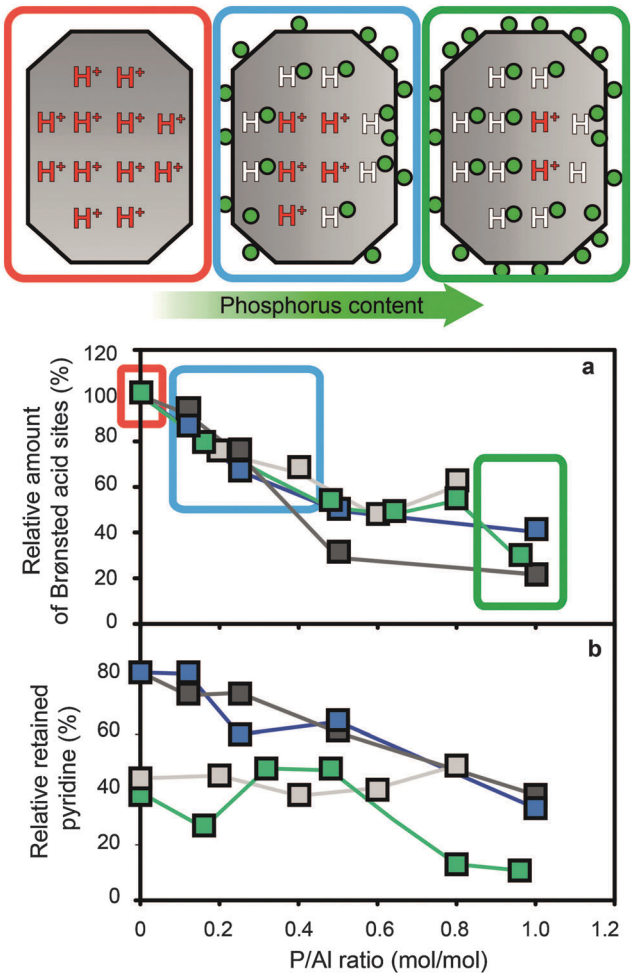

Fig. 6 (a) Relative amount of Brønsted acid sites *vs.* P/Al ratio, as determined by adsorption of pyridine at 150 °C. The concentration is relative to the parent material. (b) Relative acid site strength of Brønsted acid sites *vs.* P/Al ratio, as determined by adsorption of pyridine at 150 °C and 350 °C. The percentage is the concentration of protonated pyridinium ions of a sample at 350 °C, divided by the concentration of protonated pyridinium ions of the same sample at 150 °C. ■ = H-ZSM-5 + $NH_4H_2PO_4$ (Si/Al = 15) ■ = H-ZSM-5 + $NH_4H_2PO_4$ (Si/Al = 25) ■ = H-ZSM-5 + H_3PO_4 (Si/Al = 25) ■ = H-ZSM-5 + $NH_4H_2PO_4$ (Si/Al = 40). Data obtained from the work of Blasco *et al.*[34]

loading is understandable.[56,58,59,82,87] Also, the expected formation of neutral local SAPO interfaces will decrease the overall negative charge on the zeolitic framework, which reduces the amount of protons that can act as counter-cations.

In the literature it is reported that with weight loadings of phosphorus above 5 wt% strong acid sites have almost completely disappeared.[35,68,77,81] The Brønsted/Lewis acid site ratio is found to decrease in samples modified by phosphorus, which would indicate that Lewis acid sites are not as much affected by phosphorus as Brønsted acid sites.[35,64,76,86,91,96,100,102]

However, introduction of phosphorus without any thermal treatment also leads to a decrease in strong acid sites.[50,67,86] This decrease is completely reversible, as washing the sample leads to full recovery of all strong acid sites without any signs of permanent dealumination.[50,86] Furthermore, it was calculated

that after thermal treatment the number of Brønsted acid sites does not correspond to the amount of tetrahedrally coordinated framework aluminium (TFAl) species in phosphated samples.[67,92] In other words, 20% more TFAl species were present than Brønsted acid sites. When the sample was mixed with alumina or washed with hot water, these phosphorus species reacted and 20% of Brønsted acid sites were recovered.[67,92] The recovery of acid sites after thermal treatment by washing with hot water was confirmed in other studies.[36,67,85,86]

It is important to understand from the former results that phosphorus is not only a dealuminating agent, but reduces the number of Brønsted acid sites in a reversible way. Therefore, although breaking of Si–O–Al bonds and the formation of local SAPO interfaces during SAPO-fication are reasons for permanent loss of acid sites, reversible interactions of phosphorus with framework aluminium as described in Section 3.1.2 lead to a reversible loss of acid sites as well. At this moment the exact nature of the reversible loss of acid sites is not well understood, but a recent computational study suggested that hydrogen bonding between orthophosphoric acid and framework oxygen could lead to the formation of a $H_3PO_4H^+$ group, similar to a suggestion of Blasco *et al.*[34,103] We are hopeful that future computational studies will elucidate the origin of reversible acid loss in phosphated zeolites.

3.2.4 Decrease in acid site strength. Phosphorus modification of zeolites not only decreases the number of acid sites, but also decreases the average acid site strength.[29,31,33–36,50,53,54,57,60,63,64,66–69,74,76–78,81–86,94,102,110,116,128,129,132,133] Generally, it is reported that the average acid site strength decreases with an increase in the amount of phosphorus, as can be seen in Fig. 7a and b. These observations originate from three effects.

First of all, the maximum temperature at which molecules of probes are desorbed from bridging hydroxyl groups shifts to lower temperatures with an increase in phosphorus content, which indicates that these sites exhibit a decrease in acid site strength.[29,31,34,35,50,53,54,57,63–65,74–77,85–87,90,91,94,102,110] Theoretical calculations have indicated that intermolecular bonds between phosphoric acid and the zeolitic framework lead to a decrease in acid site strength.[103] Conversely, rates of H/D exchange for propene and adsorption of acetonitrile indicated that the remaining acid sites in H-ZSM-5 modified by phosphorus were not altered in their acid site strength.[59,89]

Secondly, relatively more strong acid sites are affected by phosphatation than weak acid sites. The corresponding increase in the ratio of weak/strong acid sites leads to an overall decrease in the average acid site strength.[31,50,53,63,64,68,69,75–78,82,83,85,91,94,116,128,129,133]

Thirdly, there have been reports where the number of weak acid sites actually increases.[35,50,54,57,81,84,90] The formation of these new weak acid sites has been attributed to the formation of P–OH groups, hydrogen-bonded Si–OH groups in silanol nests and framework-incorporated phosphate species.[35,50,54,57,94] With weight loadings of phosphorus above 2 wt%, P–OH groups and internal Si–OH groups have been observed.[34,53,54,56,64,82,86,89,92,94,96,107,134] It has been reported that these P–OH groups are able to protonate pyridine.[34,54] In contrast, Rahman *et al.* reported that P–OH groups have no acidic character and attributed the sites to excess phosphates.[96,97] Other attributions have been P–OH groups in framework-incorporated phosphate species and orthophosphoric acid.[56,58,87,92,94] Nevertheless, at this moment the nature of the weak acid sites that form in phosphated zeolites remains elusive. Systematic studies on these new acid types should be performed in order to attribute them to specific acid sites.

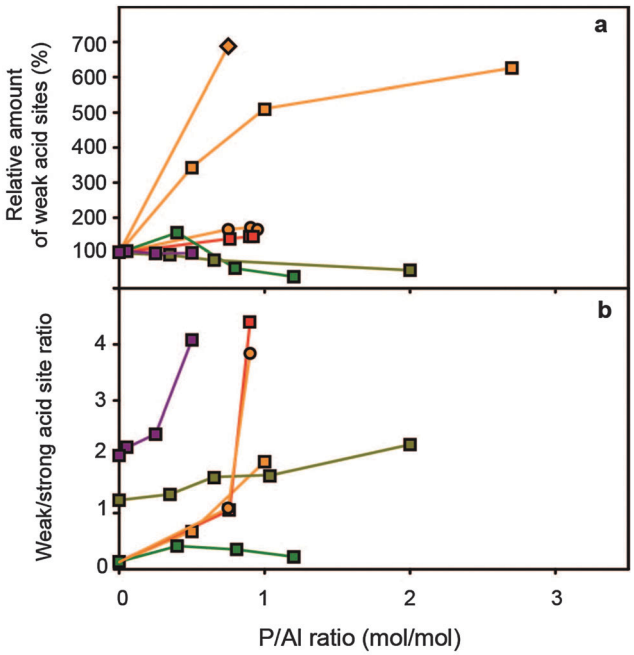

Fig. 7 (a) Relative concentration of weak acid sites (%) *vs.* P/Al ratio (b) weak/strong acid site ratio *vs.* P/Al ratio. Concentrations are relative to the respective parent H-ZSM-5 material. ■ = Rumplmayr *et al.*[91] precursor: TMP, probe: pyridine, ■ = Vinek *et al.*[90] precursor: □ = H_3PO_4, ○ = TMP, ◇ = TMPT, probe: pyridine ■ = Jiang *et al.*[76] precursor: $(NH_4)H_2PO_4$, probe: NH_3 ■ = Lee *et al.*[78] precursor: H_3PO_4, probe: NH_3, ■ = Caeiro *et al.*,[33] precursor: H_3PO_4, probe: *n*-propylamine.

4. Hydrothermal stability

As mentioned in the introduction, hydrothermal stabilisation of zeolites is a topic of extreme importance for their use in future clean/green chemical processes. Therefore, we dedicate a separate section of this review paper to the promotional role that phosphorus plays in hydrothermal stabilisation of zeolites.

4.1 Hydrothermal stability of zeolites

Zeolites are metastable, as they form under hydrothermal conditions as a transitional phase of quartz.[135] Therefore, the continued application of hydrothermal conditions eventually leads to the collapse of their framework structure. In the presence of steam and at temperatures above 400 °C framework Si–O–Al bonds will be gradually hydrolysed and aluminium will be expelled from the framework, forming extra-framework aluminium (EFAl) species (Scheme 3).[104,105,136–138] During this process, silicon can also be extracted from the framework,

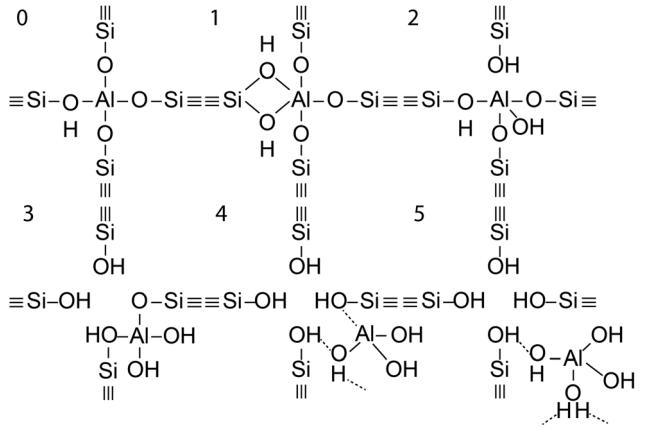

Scheme 3 Reaction steps with intermediate configurations found for dealumination. A solid line is a covalent bond. A dashed line is a hydrogen bond. Based on Malola *et al.*[105]

leading to the formation of extra-framework silica-alumina.[139] When Si and Al atoms are extracted from the zeolite lattice, mesopores form and amorphisation of the crystal lattice can take place.[5,137] Due to the removal of negatively charged $[AlO_4]^-$ units from the zeolite lattice, this so-called dealumination will reduce the amount of counter-cations that the zeolitic framework can retain. In the case of H-zeolites, this means that the active sites for catalysis are lost.[140]

The exact nature of extra-framework aluminium is not clear, but it has been shown to consist of four-, five-, and six-coordinated aluminium species.[137,141] Furthermore, it has been suggested that extra-framework aluminium can be cationic and can replace protons in bridging hydroxyl groups.[142,143] The hydrothermal stability of a zeolite indicates how prone the framework is to dealumination under hydrothermal conditions. Therefore, a zeolite that does not undergo dealumination and retains acid sites during treatment by steam exhibits high hydrothermal stability. The hydrothermal stability of a zeolite depends on the number of aluminium atoms in the lattice, the framework type, and the type of counter-cations.[137,144] Increases in temperature, the volume of steam, or the duration of hydrothermal treatment all lead to more severe dealumination.[145,146]

As briefly mentioned in the introduction, dealumination poses a challenge to the industrial application of zeolites as acid catalysts. For example, in the FCC process a regeneration step of zeolites is performed at high temperatures and in the presence of steam.[25] Although this step is effective in the removal of coke deposits, dealumination induced by steam leads to gradual permanent deactivation of the catalyst.[25,140] This catalytic deactivation of zeolites will also take place in high-temperature reactions in which H_2O will form as a reaction by-product, examples being the methanol-to-hydrocarbons (MTH) process and the dehydration of alcohols.[61,62] Therefore, hydrothermal stabilization is essential for the industrial application of zeolites.

For zeolite Y, the most important cracking catalyst, rare-earth cations and ultra-stabilization by hydrothermal treatment are used to stabilize the material.[147,148] In MCM-41, hydrothermal stabilization can be achieved by the addition of salts during synthesis.[149,150] In the case of zeolite H-ZSM-5, hydrothermal stabilization can be achieved by the addition of phosphorus.[27,33,34,50,58] Therefore, most of the studies on stabilization induced by phosphorus have been performed on H-ZSM-5, although it has been found that zeolite IM-5 can be stabilized by phosphorus as well.[127]

4.2 Promotion of hydrothermal stability by phosphorus

4.2.1. Acid sites. Removal of aluminium from the framework during steaming conditions leads to a loss of active sites. Hydrothermal treatment at temperatures above 750 °C and for longer than 5 h leads to almost complete disappearance of the bridging hydroxyl groups in zeolites.[34,58,107] After hydrothermal treatment of phosphated zeolites, it has generally been found that Brønsted acid sites are (relatively) better retained in samples modified by phosphorus than in their non-phosphated counterparts.[33,34,50,51,57,58,78,85,107,127] If the steam treatment is mild in temperature or lasts a short time, the total decrease in the number of acid sites is relatively low in comparison with non-phosphated samples. However, the absolute number of acid sites is still lower for samples that were phosphated and then steamed than for the parent and steam-treated samples.[33,50] This effect was also observed at high weight loadings of phosphorus above 3.5 wt%[85] and is because the phosphatation step has already led to an initial decrease in acid sites as described in Section 3.2.3.

If steam treatment is more severe, a higher absolute number of acid sites remain for phosphated H-ZSM-5.[33,34,50,51,57,58,78] The phosphorus content plays a role as increasingly higher loadings lead to an increasingly higher number of acid sites being retained after steaming.[34,51] However, optimal loadings of phosphorus have been reported, which lead to a maximum number of strong acid sites being retained as can be seen in Fig. 8.[33,34,78] The corresponding P/Al ratios that were reported are different, *i.e.*, 0.5, 0.65 and 1. However, the weight loadings are somewhat more similar, *i.e.*, 1.3 wt%,[78] 1.4 wt%,[33] and 2 wt%.[34] The reason for the optimum number of retained strong acid sites most likely stems from the two effects of phosphorus on zeolite H-ZSM-5, *i.e.*, the progressive decrease in acid sites with an increase in phosphorus loading on the one hand and the increase in hydrothermal stability on the other.[33] This effect is schematically drawn in Fig. 8.

Generally, the number of weak acid sites is not as much affected by steam treatment as the number of strong acid sites.[33,50,51,57,64,75,78,107] This phenomenon leads to an even stronger shift towards a lower average strength of acid sites after steam treatment. Furthermore, Lischke *et al.* demonstrated the formation of a new type of weak acid site by following the decomposition of ammonium for steam-treated NH_4^+-exchanged P/NH_4-ZSM-5 samples. Washing with hot water did not remove this new weak type of Brønsted acid site, but washing with HNO_3 could. The authors attributed the newly formed type of weak acid site to surface-bonded phosphoric acid species, which cannot be removed by washing with hot water.[50] This type of weak acid site was confirmed in another work and also attributed to (pyro)phosphoric acid.[33]

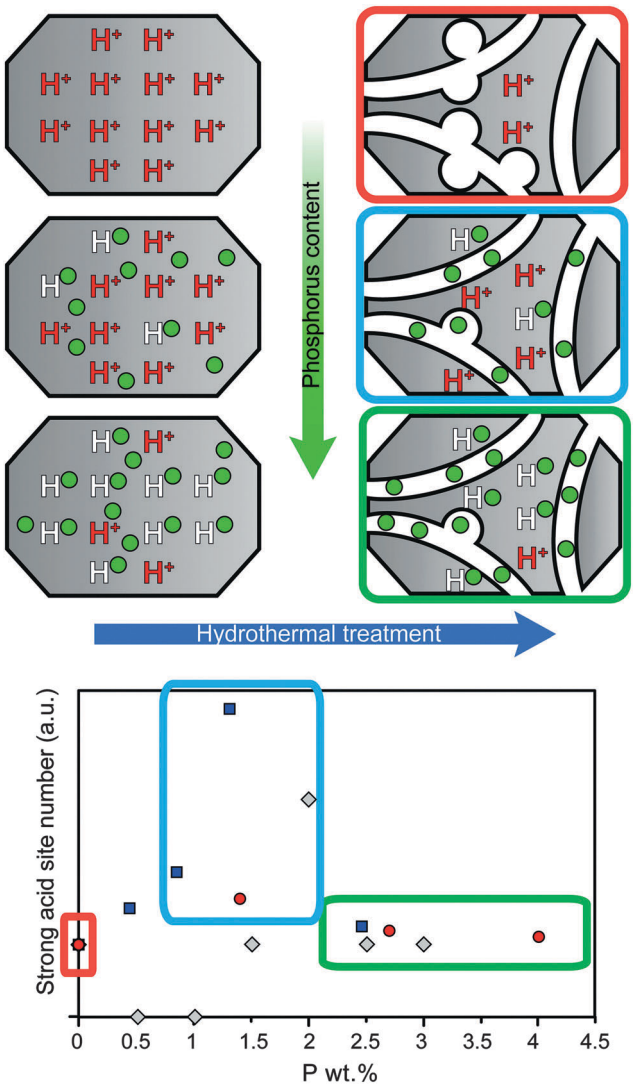

Fig. 8 Schematic representation of the promotional effect on the number of acid sites during hydrothermal treatment with increasing weight loading of phosphorus. The number of strong acid sites is normalized to the amount of acid sites in the parent material after hydrothermal treatment. ■ = Caeiro *et al.*[33] ■ = Lee *et al.*[78] ■ = Blasco *et al.*[34]

4.2.2. Porosity. The (relative) change in micropore volume and surface area after steaming is less for phosphorus-modified samples when compared to their non-phosphated counterparts.[33,34,78,102,107] This is in accordance with the retarding effect that phosphorus has on dealumination. There are reports of phosphated zeolites with phosphorus contents above 1 wt% in which the micropore volume and area increase after post-steam treatment.[34,57,75,78,87,107] After hydrothermal treatment of phosphated H-ZSM-5, 94% of phosphorus could be eluted by washing in NH_4F. However, the surface area and micropore volume only increased by less than 6%[19] and no increase in surface area and micropore volume was observed after washing with hot water.[85,107] These results indicate that phosphorus actually prevents the destruction of micropores, instead of filling newly formed mesopores.

4.2.3. Effect of hydrothermal treatment on phosphorus species. X-ray photoelectron spectroscopy (XPS) measurements showed a 55% increase in phosphorus species on the surface of 2 wt% phosphated H-ZSM-5 after steam treatment.[51] This would indicate that phosphorus migrates to the surface during steaming. Chemical analysis has shown that 5–10% of phosphorus species disappear after hydrothermal treatment.[57] With an increase in phosphorus content, the $P_{Surface}/P_{Bulk}$ ratio decreased for hydrothermally treated samples, *i.e.*, with an increase in the weight loading of phosphorus more phosphorus was found in the bulk.[51] Unfortunately, the $P_{Surface}/P_{Bulk}$ ratios before steaming were not given in the work. However, if we keep the model from Fig. 2 in mind, the latter finding would indicate that phosphorus migrates out from and also into the zeolite, depending on the weight loading. Furthermore, results of X-ray absorption microscopy showed that phosphorus species are more homogeneously distributed after steam treatment, which indicates that phosphorus species move into the zeolite.[87] This contradiction deserves more careful study.

After post-steam treatment, the amount of smaller phosphate species decreases and the amount of more condensed polyphosphate species increases.[33,34,50,55,57,58,64,78,85] The amount of condensed species can be reduced after a washing step, which would indicate that the condensed species are either washed out or hydrolysed into smaller species.[50,59,85] Furthermore, spectroscopic results indicate that most phosphorus appears to be present at local SAPO interfaces,[33,34,50,55,57,58,64,78,85] especially for samples with P/Al ratios above 0.6.[33,34,50,55,57,58,64,78,85]

4.2.4. Stabilisation of framework aluminium. For phosphated zeolites, the decrease in the number of Si–O–Al bonds, *i.e.*, the decrease in TFAl species and formation of EFAl species during steaming, is reduced, which further confirms that phosphorus stabilizes TFAl species.[34,50,58,75,78] In two reports, the reduced decrease in the number of TFAl species during steam treatment for phosphated H-ZSM-5 was only relative when compared to non-phosphated H-ZSM-5 and the absolute number of TFAl species after steam treatment remained higher for non-phosphated samples. This was the case even for samples that were steamed under severe conditions.[33,71] It was found that migration of aluminium to the external surface decreased during steaming with an increase in the amount of phosphorus loading.[51] This indicates that phosphorus either inhibits the migration of aluminium species or prevents dealumination altogether. Several studies have shown that local SAPO interfaces are not affected by steam treatment.[33,34,55,58,71,78,85,87,107]

A recent 3-D X-ray tomography study shown in Fig. 9 indicated that local SAPO interfaces are located throughout zeolite H-ZSM-5 and hold aluminium atoms fixed in the framework, which was previously suggested by Zhuang *et al.* and Damodaran *et al.*[55,58,71] This explains why the pore structure of the zeolite remains intact during steam treatment. The study further showed that the location of phosphorus plays an important role in the phenomenon of hydrothermal stabilization. As previously discussed, phosphorus establishes a gradient and does not penetrate completely into the interior of the zeolite. Therefore, aluminium atoms that are located far from the external surface

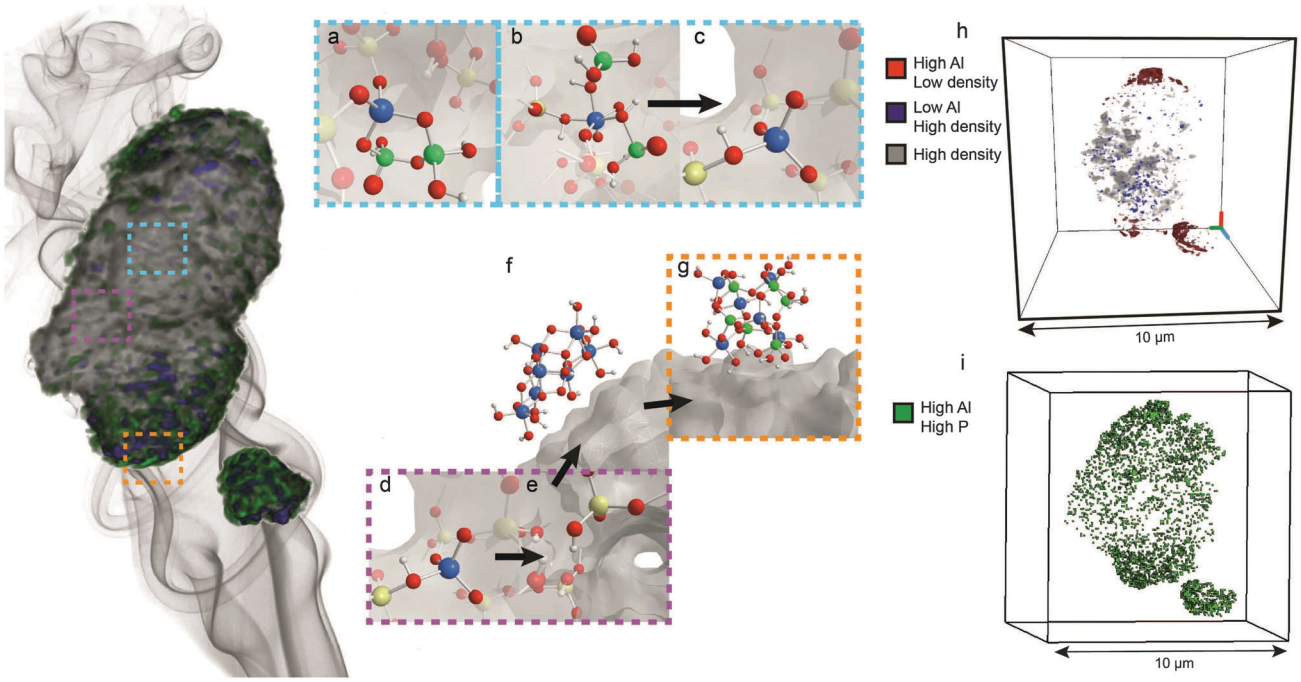

Fig. 9 Phosphated and steam-treated H-ZSM-5 sample, adapted from ref. 107 and the main effects that take place during steam treatment. (a) Local framework SAPO interfaces are not affected by steam treatment and remain in the framework. (b) Physically coordinated TFAl species are also resistant to steam, whereas (c) removal of physically coordinated phosphates by washing with hot water leads to recovery of acid sites. (d) TFAl atoms that are not interacting with phosphorus are (e) expelled from the framework and (f) migrate as AlO(OH) species to the surface, where they (g) react with phosphates to form aluminium phosphates. (h) Statistical analysis of the particle showing the presence of zones enriched in Al on the external surface and regions depleted in Al in the interior of the crystal. (i) Statistical analysis of the particle showing high concentrations of phosphorus and aluminium on the external surface, indicating the presence of extra-framework $AlPO_4$ islands that form on the surface.

will not be in the presence of phosphorus.[55,71,86,87] Consequently, these classic TFAl atoms are expelled from the framework during hydrothermal treatment.[33,34,55,71,85–87,107] High steaming temperatures and H_2O lead to migration of this extra-framework aluminium to the external surface of the zeolite, where these species react with excess phosphorus to form $AlPO_4$.[33,34,51,55,71,107,151,152] This means that phosphate species also effectively act as a sink for EFAl species, which is another possible promotional effect of phosphorus.[92] As EFAl species have been suggested to be present as debris in the pores and form cationic Al species that replace protons on bridging oxygen groups, removal of these species could explain the higher number of strong acid sites that were retained.[136,153]

The improved hydrothermal stability of H-ZSM-5 after phosphatation (or SAPO-fication) can be rationalized by the presence of local SAPO interfaces. It is well known that SAPO materials are extremely hydrothermally stable and have been reported to withstand temperatures up to 1000 °C in steam without significant loss of crystal structure.[154–156] Therefore, the formation of patches of SAPO throughout the zeolite framework reinforces its structure, keeping the framework intact during prolonged exposure to hydrothermal conditions.

Nevertheless, although phosphorus has a promotional effect on the hydrothermal stability of TFAl species, increasing the time and temperature of hydrothermal treatment eventually leads to the complete removal of aluminium species from the framework. As hydrothermal treatment gradually breaks all Si–O–Al bonds at one aluminium site, more Al–O–P bonds are formed in the presence of phosphorus.[58,71,104] For steam treatment at elevated temperatures and prolonged times the formation of an extra-framework crystalline $AlPO_4$ phase has been observed.[58,85] Crystalline $AlPO_4$ is only formed under severe steaming conditions, as $AlPO_4$ is not observed after steaming P/H-ZSM-5 at temperatures lower than 760 °C for less than 2 h.[55,58,71,87,107] However, in the case of Caeiro *et al.*, an $AlPO_4$ phase was not observed even after steaming phosphated H-ZSM-5 at 800 °C for 20 h.[33]

It is important to realise that local SAPO interfaces do not prevent dealumination during hydrothermal treatment altogether, but most likely retard the process, as shown in Scheme 3. The formation of $AlPO_4$ is gradual, as illustrated in Fig. 10.

4.2.5. Reversible decrease in acid sites after steaming. Hydrothermal treatment of H-ZSM-5 and P/H-ZSM-5 reduced the number of strong acid sites in both samples. However, it has been found that elution of phosphorus after hydrothermal treatment leads to recovery of strong acid sites. When a sample was phosphated and then post-steam treated at 700 °C for 0.5 h, the amount of phosphorus that could be removed from the sample by washing was 60%.[50] Before elution treatment of P/H-ZSM-5, the number of acid sites that remained was only 13% that of the parent material. After elution, the concentration of acid sites increased to 42% that of the parent material.

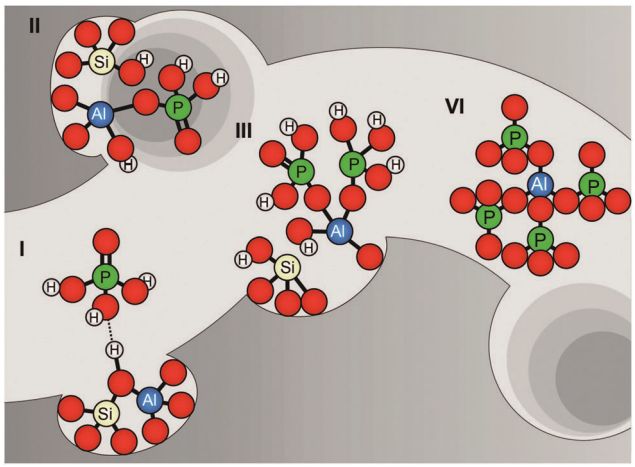

Fig. 10 Proposed model of different stages of dealumination in the presence of phosphorus. Model is based on suggestions by Abubakar *et al.*, Zhuang *et al.*, and Cabral de Menezes *et al.*[58,59,71]

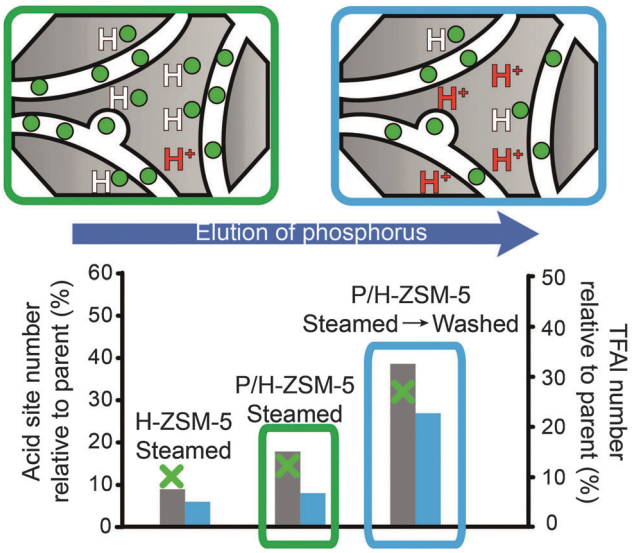

Fig. 11 Schematic representation of the recovery of the number of acid sites and TFAl species by washing after hydrothermal treatment. The acid site number is relative to the respective parent materials. Left axis: acid site number was determined using adsorption of pyridine. ■ = Lischke *et al.*[50] (steamed at 700 °C for 30 min. Washed using hot water) ■ = Blasco *et al.*[34] (steamed at 750 °C for 5 h. Washed using NH_4F) right axis: TFAl number was determined using ^{27}Al MAS NMR. ■ = Lischke *et al.* (steamed at 700 °C for 30 min. Washed using hot water).[50]

Steam-treated and washed P/H-ZSM-5 had 114% more strong acid sites than steam-treated H-ZSM-5. Other experiments on elution of phosphorus from hydrothermally treated P/H-ZSM-5 confirmed these results.[34,85,107] Acid sites in steam-treated non-phosphated materials could not be retrieved after washing with NH_4F.[34] Recovery of the number of acid sites by washing is shown in Fig. 11.

In addition, Liu *et al.* found a small quantity of a new type of strong Brønsted acid site that was formed after a steaming and washing step.[85] They reported that subsequent steam treatment removed the acid site, whereas a further washing step caused it to reappear. Similarly to the recovery of acid sites after hydrothermal treatment, the amount of TFAl species that can be recovered by elution of phosphorus is much lower than before steaming.[50] Still, a considerable amount of aluminium species can be retrieved as TFAl species. That is, of the 30% of the original amount of TFAl species that remained after steaming P/H-ZSM-5 under mild conditions, 70% of the original amount of TFAl species could be obtained after washing. With increasingly severe hydrothermal treatment conditions, this amount decreased, *i.e.*, from 15% of the original amount of TFAl species after steaming to 30% of the original amount of TFAl species after washing, as shown in Fig. 11.[50] Similar results have been reported in other works.[85,107]

Although these findings are not quite understood at the moment, an important consequence of the recovery of the number of strong acid sites after washing is that the hydrothermal stabilization effect of phosphorus does not seem to require irreversible phosphorus–aluminium interactions. Recently, a study performed by our group has shown that the recovery of strong acid sites and TFAl species is accompanied by the decrease in lattice aluminium that was attributed to six-coordination by phosphates.[85,107] These findings indicate that TFAl atoms, which adopt six-fold coordination in the presence of phosphate species, are hydrothermally stabilized as well.

4.2.6. Only for zeolite H-ZSM-5? As mentioned, local SAPO interfaces have been found to remain unaffected during steam treatment and, as aluminium remained fixed in the framework, the pore structure was better retained. However, with prolonged steam treatment all Si–O–Al bonds at SAPO interfaces are eventually hydrolysed, leading to the formation of extra-framework $AlPO_4$.[58] Therefore, it would seem that SAPO interfaces form metastable intermediates during dealumination in the channel system of zeolite H-ZSM-5. We explicitly mention the channel system of zeolite ZSM-5, as it is not certain if phosphorus has a similar promotional effect on very different framework topologies. In a contribution from Costa *et al.* it can be seen that for zeolite H-beta and H-mordenite phosphatation followed by hydrothermal treatment only leads to the formation of extra-framework crystalline $AlPO_4$.[30] Authors from the same group applied a similar steam treatment to phosphated H-ZSM-5 and spectroscopic signatures of SAPO interfaces could be seen.[33] This raises the question whether local SAPO interfaces in H-ZSM-5 are inherently stabilized by the MFI channel system, but not in other topologies, where only extra-framework $AlPO_4$ would form. It could explain why reports in the academic and patent literature on phosphorus modification are almost exclusively based on zeolite H-ZSM-5 or similar multidimensional 10-MR structures, such as ZSM-11, MCM-22, ITQ-13 and IM-5.[82,110,112,127] Already, the phosphatation of intergrowth structures of ZSM-5/ZSM-11 led to higher dealumination rates after phosphatation than with H-ZSM-5.[82] On the other hand, it has been reported that modification by phosphorus of the mesoporous material MCM-41 led to significant hydrothermal stabilization.[157] We hope to see future systematic studies that will shed new light on these scientifically pertinent questions. Computational studies such as those performed by Svelle *et al.* and Lisboa *et al.* could shed new

light on the actual stabilizing effect that the proposed phosphorus–aluminum interactions produce on the framework.[104,138,158]

5. Phosphorus and zeolite-based catalysis

In the previous sections we have shown that phosphorus affects the acidity, porosity and hydrothermal stability of zeolites. As expected, this has a profound effect on the catalytic properties of zeolites in a variety of catalytic processes, as can be seen in the following sections. However, since catalytic conditions and materials differ in most of the literature, direct comparisons concerning performance are almost impossible to make. Therefore, all comparisons and figures in the following section are only meant to show rough trends and the reader should keep it in mind that differences between, *e.g.*, reaction temperature, conversion, Si/Al ratio, crystal size and space velocity have not been taken into account.

5.1 Automotive catalysis

Transition metal-exchanged zeolites are used in automotive catalysis to remove NO_x formed during the combustion of transportation fuels and are especially suited for diesel engines.[4,37,159] The process is known as ammonia selective catalytic reduction (NH_3-SCR) and examples of catalysts are Fe-ZSM-5, Fe-beta and Cu-SSZ-13, although small-pore zeolites such as SSZ-13 were found to be most active.[4,37,65] In short, NO is oxidised to NO_2 by transition metal ions (TMI), *e.g.*, Fe^{3+} and Cu^{2+}, which act as redox centres.[159,160] When NO or NO_2 reacts with NH_3 chemisorbed on Brønsted acid sites, N_2 and H_2O are formed.[159,160]

Deactivation of NH_3-SCR zeolite catalysts during operation occurs mainly due to thermal conditions and chemical poisoning.[4] Although many chemicals present in the feed, *e.g.*, Pt, Zn, and Ca, poison the catalyst, poisoning by phosphorus is especially damaging.[37,161] Phosphorus compounds are present in lubricant oils and biofuels and come into contact with the zeolite catalyst during operation.[65] NH_3-SCR zeolites that are treated with phosphorus show a strong decrease in nitrogen oxide-removing activity.[32,37,65,161] It was found that there is a linear relationship between phosphorus content and decrease in catalytic activity.[32]

Effective poisoning with phosphorus is caused by several deactivation mechanisms, which are related to the previously discussed physicochemical changes induced by phosphorus.[37] First of all, there is a decreased amount of NH_3 that can be chemisorbed.[32,37,65,161] This can be attributed to a loss of acid sites and to blocking of active sites by phosphate species. However, it was found that the decrease in NH_3 uptake was only minor compared to the decrease in chemisorbed NO and NO_2 species and is therefore only a partial contributor to deactivation of the catalyst.[65,161]

The decrease in chemisorbed NO_x species indicates that there is a decrease in TMI centres, which was confirmed by an increase in Fe^{2+} and CuO species after the introduction of phosphorus.[37,65] Furthermore, it was found that after modification

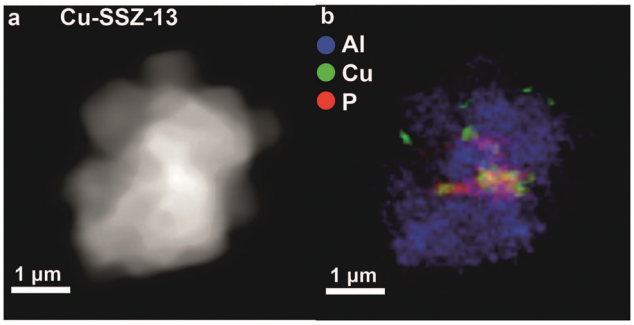

Fig. 12 X-ray absorption microscopy results for a Cu-SSZ-13 crystal agglomerate poisoned by phosphorus (0.34 mmol g^{-1} zeolite). (a) Density map. (b) Elemental map. It can be seen that phosphorus and copper are located on the external surface of the agglomerated squares. Adapted from ref. 37.

by phosphorus Fe^{2+} could not be reduced to Fe^0 at low temperatures.[161] In the case of Fe, it was suggested that Fe^{3+} reacts with phosphorus.[65,161] However, another explanation of the observed effects was suggested to arise from partial dealumination caused by phosphorus.[37] In this manner the negative charge on the framework decreases and Cu^{2+} countercations are forced into CuO agglomerates. It was further observed that these CuO agglomerates moved out of the zeolite and were deposited on the external surface, as can be seen in Fig. 12.[37] Their presence was suggested to decrease the accessibility of the material even more. While further studies should be performed to determine the exact effect of phosphorus–TMI interactions, the decrease in acid sites, dealumination and pore blocking all follow from previously discussed phosphorus–zeolite interactions. The attraction between phosphorus and framework aluminium and the formation of neutral SAPO interfaces are good explanations why phosphorus is a much more effective poison than Zn, Pt, and Ca.

5.2 Hydrocarbon catalysis

Protonation by Brønsted acid sites of C–C bonds, C–H bonds, or –OH groups in hydrocarbons and alcohols leads to the formation of carbonium, carbenium, or oxonium groups.[162–164] Subsequently, these groups can be cracked, dehydrogenated, dehydrated, isomerised, or oligomerised. As H-zeolites have Brønsted acid sites and shape-selective properties, they are widely used in industry in these types of reactions to produce hydrocarbons. Changes induced by phosphorus in the number and strength of acid sites and shape selectivity lead to different catalytic properties. Furthermore, the catalytic lifetime is increased as the hydrothermal stability increases for phosphated materials.

5.2.1 Effect of acid site loss. The decrease in the number and strength of acid sites caused by phosphatation has obvious effects on hydrocarbon catalysis performed by zeolites. It can be expected that a reduction in Brønsted acid sites, *i.e.*, the active sites in acid-catalysed reactions, leads to a decrease in catalytic activity. Certainly, this effect can be observed for several hydrocarbon catalysis processes as shown in Fig. 13a and b, as the progressive reduction in the number of Brønsted acid sites with

an increase in phosphorus content leads to a decrease in activity in the catalytic cracking of hydrocarbons,[33,34,57,64,76,79,85,90,97,99,110,127] dehydration of alcohol[20,21,24,38] and methanol-to-hydrocarbon reaction.[29,31,59,67,82,96,97,112]

For the cracking of alkanes, it was established that there is a linear correlation between a high number of Brønsted acid sites and cracking activity in phosphated zeolites.[33,90] In the cases of the methanol-to-hydrocarbons reaction and dehydration of alcohol, 100% conversion can be obtained with an increase in temperature.[29,31,59,67,77,81–84,96,97,112] For the MTH reaction these results are not surprising as Hunger *et al.* showed that zeolite materials with a very low number of Brønsted acid sites could achieve 100% conversion of methanol at 400 °C.[165]

Besides activity, a decrease in the number of acid sites can change the selectivity in hydrocarbon catalysis reactions as well, provided that it reduces the chance of secondary reactions. This is shown in Fig. 13c and d. For the MTH reaction, selectivity towards light olefins and especially propylene increases for unmodified zeolite materials with a low number of acid sites.[31,59,112,165–167] It has been suggested that a low density of acid sites reduces the chance of the primary MTH products (light olefins) undergoing hydride transfer and cyclisation reactions during diffusion, thus decreasing the formation of larger products.[31,167,168] In agreement with this, the observed decrease in strong acid sites in phosphated zeolites leads to improved selectivity toward light olefins in the MTH reaction.[29,31,59,67,82,96,97,112] In Fig. 13d it can be observed that the selectivity towards light olefins increases with an increase in phosphorus loading, *i.e.*, a decrease in the number of acid sites.

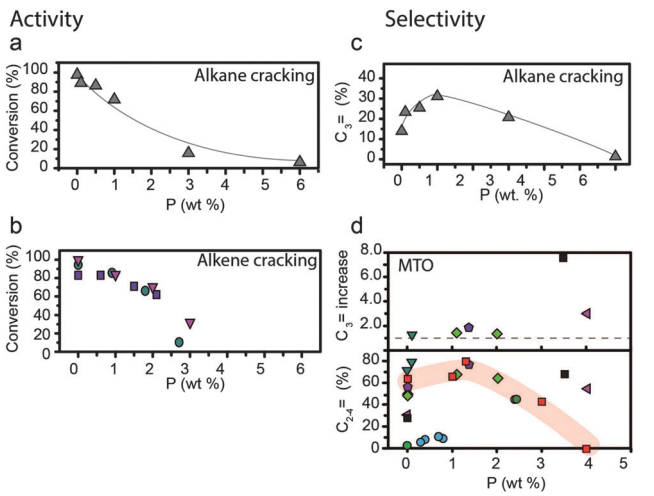

Fig. 13 Effect of weight loading of phosphorus on (a) alkane cracking activity, conversion of reactant.[76] (b) Alkene cracking, conversion of reactant. ■ = Zhao *et al.*[64] ■ = Xue *et al.*[57] ■ = Xue *et al.*[79] Differences between reaction temperature, Si/Al ratio, crystal size and space velocity have not been taken into account. (c) Alkane cracking selectivity, selectivity for propylene (%)[76] (d) (top) methanol-to-olefins (MTO) selectivity, increase in selectivity for propylene. The increase in selectivity for propylene is relative to that of the respective parent material. (d) (bottom) Actual C_2–C_4 selectivity *vs.* weight loading of phosphorus in MTO. ■ = Kaeding *et al.*[52] ■ = Rahman *et al.*[96] ■ = Rahman *et al.*[97] ■ = Védrine *et al.*[29] ■ = Abubakar *et al.*[59] ■ = Liu *et al.*[31] ■ = Li *et al.*[82] ■ = Dyballa *et al.*[89] The red highlight focuses on a trend in optimum loading of phosphorus reported in ref. 89. Reaction temperatures are between 400 °C and 460 °C. Differences between Si/Al ratio, crystal size and space velocity have not been taken into account.

It is expected that the decrease in the number of acid sites also influences the product selectivity in catalytic cracking of alkanes. Catalytic cracking over zeolites with a low number of acid sites generally follows the protolytic cracking route (monomolecular mechanism).[169] This is because a low density of acid sites reduces the chance of alkanes reacting with carbenium ions (bimolecular mechanism).[170] The bimolecular mechanism is in essence a secondary reaction of the monomolecular pathway, as carbenium ions are formed in the latter.[162,163,171,172] For more information on monomolecular and bimolecular cracking mechanisms we refer the reader to some of the excellent reviews that have been written on the subject.[162,163,171,172]

Nevertheless, typical products that are formed by the monomolecular cracking mechanism are methane, ethane, propylene, hydrogen and high olefin/paraffin ($C^{=}/C$) product ratios,[163,169] whereas the bimolecular cracking mechanism produces more paraffins, less olefins and more branched C_{4+} products. Therefore, phosphated materials are expected to yield a product distribution that corresponds to the monomolecular cracking mechanism. Indeed, as can be seen in Fig. 13c, phosphated zeolites applied in alkane cracking display increased selectivity towards light olefins.[33,76,85,97,101,107] However, when high alkane cracking temperatures are applied, *i.e.*, above 650 °C, product distributions are very similar for phosphated and unmodified H-ZSM-5, as at these high temperatures carbenium ions become unstable and the monomolecular mechanism is dominant.[171,173]

5.2.2 Effect of weak acid sites. A decrease in the average strength of acid sites is not expected to have a strong influence on the product distribution in the methanol-to-hydrocarbon reaction and catalytic cracking of alkanes.[1,171] Although weak Brønsted acid sites are able to crack alkanes, they were found to have turnover frequencies that were three orders of magnitude lower than those found for strong Brønsted acid sites.[90] In a study by Bleken *et al.*, no significant effect of acid site strength was found on the product distribution in the MTH reaction.[174]

However, the formation of weak acid sites does have a pronounced effect on catalytic performance in the cracking of alkenes and dehydration of alcohols. For the cracking of alkenes, modification of zeolites with phosphorus leads to an increase in propylene product yield.[57,64,66,79,102,110] Lin *et al.* showed in their study that the weak acid sites that form during phosphatation prefer a different reaction pathway to strong acid sites, which leads to higher yields of propylene.[66] Higher loadings of phosphorus, *i.e.*, a lower average acid site strength, lead to higher selectivity toward propylene.[66] However, as can be seen in Fig. 14b, the selectivity towards propylene decreases when weight loadings of phosphorus reach above 2 wt%.[57,64,79,102]

For the dehydration of alcohols, the selectivity towards ethylene increases with increases in phosphorus content and reaction temperature, as shown in Fig. 14a.[63,77,81,83,84,175] If all strong acid sites are removed, at weight loadings of phosphorus above 3 wt% the selectivity towards ethylene reaches 99.4% as only dehydration takes place.[63,77,81,83,84] If the catalyst still

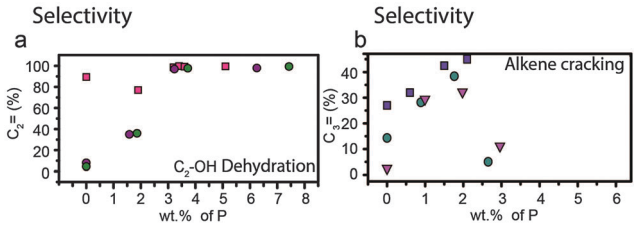

Fig. 14 Effect of weight loading of phosphorus on (a) dehydration of ethanol and selectivity for ethylene at temperatures >400 °C ■ = Zhang *et al.*[77] ■ = Ramesh *et al.*[81] ■ = Ramesh *et al.*[84] Differences between reaction temperature, Si/Al ratio, crystal size and space velocity have not been taken into account. (b) Alkene cracking and selectivity for propylene (%). ■ = Zhao *et al.*[64] ■ = Xue *et al.*[57] ■ = Xue *et al.*[79] Differences between reaction temperature, Si/Al ratio, crystal size and space velocity have not been taken into account.

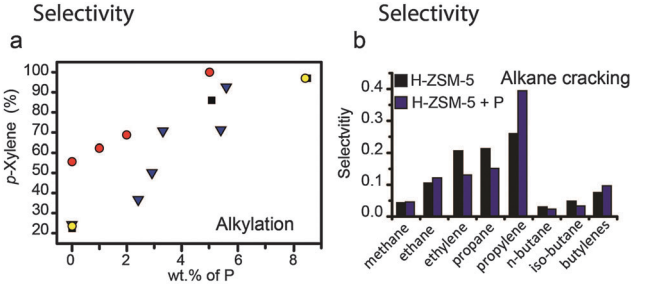

Fig. 15 Effect of weight loading of phosphorus on (a) alkylation of toluene, selectivity for *p*-xylene (%). ■ = Chen *et al.*[10] ■ = Young *et al.*[16] ■ = Kaeding *et al.*[17] ■ = Vinek *et al.*[90] Differences between reaction temperature, Si/Al ratio, crystal size and space velocity have not been taken into account. (b) Alkane cracking, selectivity in moles for the main products formed during the catalytic cracking of *n*-hexane over a full temperature program ■ = H-ZSM-5 ■ = phosphated steam-treated and eluted H-ZSM-5. Adapted from ref. 107.

contains a small amount of strong Brønsted acid sites, higher hydrocarbons are also detected. At weight loadings of 1.3–1.9 wt% P the selectivity towards propylene has been reported to reach a maximum and can be as high as 33% at temperatures between 400 °C and 500 °C.[63,81,84,175] Selectivity for propylene is maintained with time on-stream, whereas the unmodified material gradually loses selectivity.[63]

In a summary of the effect of changes in acidity on catalysis, a decrease in the number of acid sites has a promotional effect on the selectivity of the methanol-to-hydrocarbons reaction toward light olefins, especially propylene. A decrease in the strength of acid sites improves the pure dehydration of alcohols to olefins. For the cracking of hydrocarbons, decreases in both the strength of acid sites (alkenes) and number of acid sites (alkanes) lead to increased selectivity towards light olefins, especially propylene.

5.2.3 Changes in shape selectivity. So far, one can wonder whether the addition of phosphorus does anything more than decrease the number and strength of acid sites and if an unmodified zeolite with similar acidic properties is just as effective in altering catalytic performance. However, the addition of phosphorus changes zeolites – and specifically H-ZSM-5 – in an even more profound way, *i.e.*, it changes the shape selectivity. This is because of the presence of phosphates in the micropore channel system, where they form barriers to diffusion and inhibit the formation of voluminous (intermediate) species.

This effect is especially obvious in the alkylation and disproportionation of aromatics, as shown in Fig. 15a. The addition of phosphorus to H-ZSM-5 boosts the selectivity towards *p*-xylene to 95%.[10,17,36,70,90,93,95] In general, the increase in selectivity can be attributed to the effective reduction in channel pore sizes, channel intersections and pore openings.[10,17,95] Bulkier *o*- and *m*-xylenes will diffuse more slowly out of the pores and the rapid decrease in the concentration of *p*-xylenes will promote the isomerization of the former two isomers into the latter. In a recent work by Janardhan *et al.* it was found that washing out excess phosphorus from the pores improved the activity in alkylation and disproportionation of aromatics, as pore blocking was reduced. However, the selectivity remained 95% for *p*-isomers. This indicates that phosphates that are irreversibly connected to the framework are responsible for a decrease in pore volume, which restricts the formation and diffusion of the bulkier *ortho* and *meta* isomers.[36]

The presence of phosphates in the zeolite channels also has an effect on the product distribution in alkane cracking and the methanol-to-hydrocarbon reaction. If one compares the product distributions using phosphated multidimensional 10-MR zeolites in the methanol-to-hydrocarbon reaction at 400 °C it can be observed that there is an increase in selectivity for alkenes, a decrease in selectivity for aromatics and an increase in C_{3+} species.[29,52,59,82,112] The strong decrease in aromatic species is not observed for zeolites with a low number of acid sites and can therefore be attributed to the presence of phosphorus species.[59] Interestingly, similar product distributions were reported for the methanol-to-olefins reaction over zeolite H-ZSM-22, which has a 1-dimensional pore system and no channel intersections.[176] In the latter topology a decrease in selectivity for ethylene was also observed, which can also be found in the studies of Kaeding *et al.*[52] and Abubakar *et al.*,[59] but not in other works. Nevertheless, an important suggestion to make is that although modification by phosphorus alters the acidity of zeolites, it appears that a change in topology plays a major role in their selective properties as well, especially reducing the presence of aromatics in the product stream.

In a recent study performed by our group we found that the product distribution for the cracking of *n*-hexane over phosphated H-ZSM-5 resembles that for zeolites that are 1-dimensional along 10-membered ring (MR) channels, such as H-ZSM-22 and H-ferrierite.[107,177,178] Similarly to these materials, an increase in selectivity for methane, ethane, propylene, and butylene and a decrease for ethylene, butane and pentane was observed, as can be seen in Fig. 15b.

As mentioned in the previous section, this shift in the product distribution for alkane cracking is typical when the monomolecular cracking mechanism becomes dominant.[163] The change in the product distribution in the MTH reaction stems from a larger contribution from the alkene cracking cycle.[1,176] This change in mechanism in both catalytic processes stems

from the same origin. More specifically, the change in selectivity arises from the ability of a zeolitic framework to stabilize carbenium ions, which are the intermediate species in the bimolecular cracking mechanism and the aromatic-based cycle in MTH.[1,163,171,176] In unmodified multidimensional medium-pore zeolites, the channel intersections can more successfully stabilize these voluminous carbenium ions.[169,171,179] However, phosphates – presumably connected to local SAPO interfaces – that are present in the channel intersections will hinder the formation of voluminous carbenium ions. This can be observed in one study on H-MCM-22, where, after modification by phosphorus, a decrease in the formation of enyl carbenium ions is observed during the MTH reaction.[112]

In summary, it is plausible that the presence of phosphate species suppresses the aromatic-based hydrocarbon pool mechanism during the MTH process, whereas in the catalytic cracking of alkanes the bimolecular cracking mechanism is inhibited. Whether this is considered a promotional or poisonous effect of phosphorus depends on the desired product distributions.

5.2.4 Improved catalytic stability. The addition of phosphorus to zeolites has been reported to lead to a decrease in the formation of coke in hydrocarbon catalysis.[31,63,64,77,81,84,107] It is expected that the decrease in the number and strength of acid sites reduces the chance of products undergoing hydride transfer and cyclisation reactions.[31,63,77,81,84] Moreover, as the formation of carbenium ions is inhibited due to a low number of acid sites and steric constraints, formation of coke is expected to decrease.[171,180,181] Not surprisingly, the decrease in the formation of coke leads to an increased catalytic lifetime.[31,64,77]

However, the major reason for the increased catalytic lifetime is the improved hydrothermal stability induced by phosphorus. After hydrothermal treatment, samples modified by phosphorus have higher catalytic activities than their non-phosphated counterparts.[33,34,57,60,64,75,78,79,85,88,107,173] If reactions are performed under hydrothermal conditions, phosphated catalysts maintain activity for a longer time on-stream.[60,63,64,88,127,175] Samples from which phosphorus was eluted after steaming regained strong acid sites and consequently their cracking activity increased.[34,85,107]

As we have seen in Section 4.2, phosphated zeolites are expected to perform better in catalysis after steam treatment than their non-phosphated counterparts, because they contain more strong acid sites. However, the direct link between the number of strong acid sites and cracking activity is not as straightforward after hydrothermal treatment. Samples with high weight loadings of phosphorus and a higher number of strong acid sites after hydrothermal treatment had lower cracking activity than samples with lower weight loadings of phosphorus and a lower or equal number of acid sites.[34] Furthermore, it was found that steam-treated parent H-ZSM-5 had a higher number of Brønsted acid sites, whereas steam-treated phosphated H-ZSM-5 had a lower amount. Interestingly, the cracking activity for the latter sample was higher.[33] Therefore, other factors such as the distribution of acid sites, accessibility and limitations to the formation of coke will probably play a role.[33] In the cracking of alkenes, it was reported that hydrothermal treatment increased the activity for phosphated samples, which would indicate that the accessibility of phosphated zeolites improves after steam treatment.[57,79]

As mentioned in Section 4, adding more phosphorus is not the key to retaining more active sites after steaming, as there are several (varying) optimum loadings of phosphorus (as shown in Fig. 16a and b).[33,34,57,60,75,78,79,88] In accordance with what was discussed in Sections 3 and 4, phosphatation leads to pore blockage, reduced accessibility and a decrease in the number of acid sites, which is amplified by increasing the loading of phosphorus. Therefore, a decrease in cracking activity is expected with an increase in phosphorus content. However, after steaming the promotion of hydrothermal stability by phosphorus comes

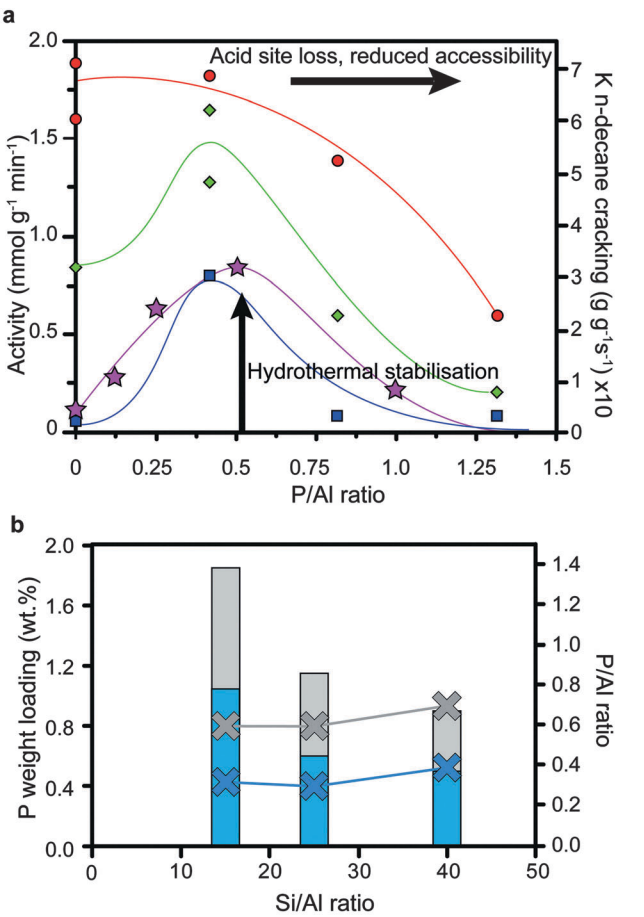

Fig. 16 (a) Effect of phosphorus and post-steam treatment on the cracking of *n*-hexane[33] (left axis) and *n*-decane[34] (right axis) by H-ZSM-5. Adapted from ref. 33. Activity is plotted against weight loading of phosphorus (H_3PO_4 precursor). Left axis:[33] ■ = H-ZSM-5 (Si/Al = 13). ■ =H-ZSM-5 steamed at 800 °C for 5 h. ■ = H-ZSM-5 steamed at 800 °C for 20 h. Reaction temperature is 500 °C. Right axis:[34] ■ = H-ZSM-5 (Si/Al = 25) steamed at 750 °C for 5 h. Reaction temperature is 500 °C. Lines are not fits and are meant to guide the eye. (b) ■ = optimal average cumulative catalytic conversion during cracking of naphtha with additional H_2O in the feed at 650 °C after 1 h for H-ZSM-5 with different Si/Al ratios *vs.* P weight loadings and P/Al ratios ($NH_4H_2PO_4$ precursor).[88] ■ = optimal first-order kinetic rate constants in cracking of *n*-decane with H-ZSM-5 steamed at 750 °C for 5 h.[34] Left axis in bars: phosphorus weight loading. Right axis as crosses with lines: P/Al ratio.

into effect. As such, when comparing a steam-treated phosphated sample with a steam-treated non-phosphated sample, the former will perform better in cracking, especially after more severe steaming conditions have been applied. The effect will decline when the phosphorus loading becomes very high, when the poisonous effects of loss of acid sites and reduced accessibility start to dominate again.[33]

5.3 Future applications

Although hydrocarbon cracking and MTH reactions are the most widely studied reactions for phosphated zeolites, there are also new promising directions where phosphated zeolites can be utilized, an example being the catalytic dehydration of bioalcohols, such as dehydration of ethanol to ethylene. As discussed in the previous sections, carrying out a phosphatation step decreases the number and strength of acid sites in a zeolite, which makes phosphated zeolites very suitable for the selective dehydration of bioalcohols to alkenes.[63,77,81,83,84] However, if these reactions are performed in the liquid phase the reversible interactions of phosphorus should be considered (Scheme 4a). The formation of H_2O during dehydration removes the reversible phosphorus–aluminium interactions and strong acid sites will reappear, leading to undesired cracking reactions (Scheme 4b). A possible solution to overcome this problem is to perform a pre-leaching step followed by post-steam treatment. In this manner, the physically interacting phosphorus is removed and the strong acid sites that form as a consequence can be removed by hydrothermal treatment (Scheme 4a–d). It is expected that this material has exclusively weak acid sites, which remain weak in aqueous environments.

Another key potential application for phosphated H-ZSM-5 is in catalytic fast pyrolysis of biomass.[2,12] In this process Ga-ZSM-5 is used to produce large amounts of aromatics from lignocellulosic biomass.[12] However, a major obstacle is the formation of coke during the process, which is overcome by thermal regeneration. Stabilization by phosphorus could be a successful method for providing additional stability during thermal regeneration. A study by Furomoto *et al.* has shown that the addition of phosphorus to Ga-ZSM-5 improves stability and suppresses carbonaceous deposits and the release of gallium from the framework during ethanol-to-propylene reactions.[182] Therefore, we hope to see future studies on the use of phosphorus as a promoter in zeolite-catalysed pyrolysis of biomass.

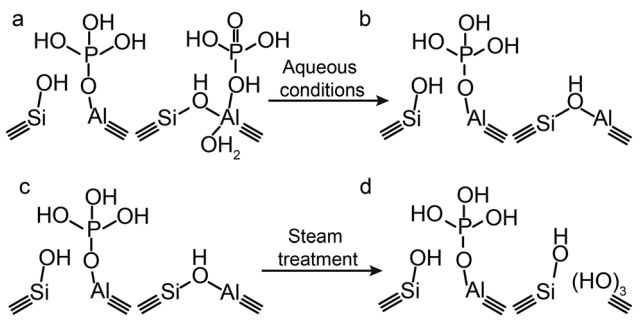

Scheme 4 Schematic representation of the effect of aqueous conditions on permanent and reversible phosphorus–aluminium interactions.

The concepts presented in this review article help the aim to modify zeolites by phosphatation more rationally. For example, by exclusive synthesis of local SAPO interfaces at channel intersections of a multidimensional 10-MR framework, one obtains a material that has a multidimensional framework structure, but not the internal cavities that promote the formation of carbenium ions. In these materials, transport of molecules is still fast, while the formation of coke and reaction mechanisms that use carbenium ions are reduced.[180,181] As the dislodged Si–O–Al–OH species that form during thermal treatment were found to act as anchoring points for phosphoric acid, thermal treatment before phosphatation is a first step in the exclusive formation of local SAPO interfaces.[86]

However, more precise synthesis methods should be explored than the impregnation methods that are often applied to introduce phosphorus.[31,33–35,50,51,53,54,56–60,63,64,66–87,90–92,107] As we have seen in the previous sections, introduction of phosphoric acid under these conditions leads to inter- and intra-particle heterogeneities. Gao *et al.* have shown that introduction of phosphorus by means of hydrothermal dispersion leads to a more homogeneous distribution of phosphorus species than by impregnation.[101,102] Janardhan *et al.* reported on the formation of phosphate monolayer islands by performing phosphatation followed by an elution step.[36] The authors argued that the removal of excess phosphorus species is essential for the creation of accessible materials. Although we agree, the elution of phosphorus by washing with hot water also removes reversible phosphorus–aluminium interactions. This can be undesirable, as is the case in the dehydration of bioalcohols. Gas-vapour deposition as a means of introducing phosphorus has been reported to lead to more phosphorus–aluminium interactions than wet impregnation.[78] Furthermore, pre-steam treatment followed by extraction of extra-framework aluminium to form mesopores could be a method of obtaining more efficient transport routes for phosphorus precursors. Extraction of extra-framework aluminium is essential in this step if the formation of extra-framework $AlPO_4$ is not desired.

Furthermore, if one were to leave the extra-framework aluminium, it is possible to synthesise an aluminium phosphate binder from the zeolite's own supply of aluminium. Especially in the field of catalytic hydrocarbon cracking, the addition of $AlPO_4$ to zeolites leads to improved selectivity for light olefins, hydrothermal stabilization, improved mechanical strength and resistance to attrition.[23,46–48,183] Furthermore, there are several arguments in favour of creating a binder phase from a zeolite's own supply of aluminium.[113] First of all, it allows the use of zeolites with low Si/Al ratios, which are cheaper and more environmentally friendly to produce, as the use of organic templates is not required.[184,185] Secondly, the formation of mesopores caused by the dealumination step creates a hierarchical material, which facilitates the access and transport of reactant and product molecules during catalysis.[186,187] Finally, careful synthesis of $AlPO_4$ from extra-framework aluminium (EFAl) allows one to form $AlPO_4$ species inside the zeolite channel/cage system, altering its shape-selective properties. Although not many studies have yet been performed in this

direction, we believe these promising avenues of phosphorus–zeolite chemistry deserve to be investigated.

On a final note, the interaction of phosphorus with zeolites could act as a model system for understanding the chemistry between zeolites and other group VA elements such as arsenic and antimony. Zeolites are very effective materials for removing arsenic from wastewater.[188–190] The suggested condensation reaction of arsenate with the Al–OH groups of surface framework aluminium has certain analogies to the formation of local SAPO interfaces.[190] Similarly to phosphorus, modification of H-ZSM-5 with antimony oxide exhibited increased *para*-selectivity in the disproportionation of toluene and a decrease in strong acid sites in H-ZSM-5.[191,192] As this type of inorganic chemistry has an effect on fields such as conversion of biomass, hydrocarbon catalysis, automotive catalysis and wastewater treatment, we hope to see future studies that explore and ultimately obtain a unified view of group VA chemistry with zeolite materials.

6. Summary

The study and comparison of the existing literature on phosphorus–zeolite chemistry has revealed many universal physicochemical effects that take place. One of the most important considerations should be that the attraction between phosphorus and aluminium is the driving force behind the physicochemical changes in phosphated zeolites, such as the decrease in the number of acid sites, decrease in framework negative charge, improved hydrothermal stability and changes in catalytic shape selectivity. Some of these changes are permanent and caused by SAPO-fication, *i.e.*, the formation of local silicoaluminophosphate (SAPO) interfaces in the zeolite framework. However, a significant other part of these changes can simply be reversed by the elution of physically bonded phosphate species. In catalysis, the physicochemical changes caused by modification by phosphorus can be either promotional or poisonous.

During the modification with phosphorus of zeolites by wet impregnation, phosphorus species are deposited on the external surface before entering the zeolite channels. Phosphorus enters the zeolite channels with increasing loadings, but limitations on diffusion lead to a distribution gradient with a higher concentration of phosphorus at the outer surface. With weight loadings of phosphorus above 5 wt%, the formation of large polyphosphates on or near the external surface is observed. Phosphorus species do not cause severe pore blockage at average loadings of phosphorus (above 2 wt%). However, treatment with phosphorus always leads to a decrease in surface area and micropore volume. This decrease is amplified with an increase in phosphorus content.

Excess phosphorus is present as ortho-, pyro-, and polyphosphates. With an increase in phosphorus content the amount of excess phosphorus increases. Excess phosphorus is dehydrated at high temperatures forming condensed polyphosphates. This effect is reversible. Rehydration leads to the formation of smaller phosphate species. Phosphorus species that do not interact with the zeolite framework can easily be eluted by washing with hot water.

Depending on the P/Al ratio and the location of phosphorus, only a certain amount of phosphorus can chemically interact with aluminium in a zeolite. Phosphorus can reversibly interact with tetrahedrally coordinated framework aluminium (TFAl) species, forcing TFAl species into octahedral coordination. Elution of phosphorus by washing with hot water reverses this effect. Phosphorus preferentially reacts with extra-framework aluminium (EFAl) or partially dislodged tetrahedrally coordinated framework aluminium ($TFAl_{dis}$) species. This leads to the formation of (amorphous) extra-framework $AlPO_4$ species and local framework SAPO interfaces. Washing with hot water cannot remove these species. Due to the lack of experimental evidence and the unstable character of Si–O–P bonds it seems unlikely that $[PO_4]$ units are fully substituted in the framework to replace $[AlO_4]$ and $[SiO_4]$ tetrahedra.

Introduction of phosphorus leads to a reduction in the number of strong acid sites. This reduction increases with an increase in the amount of phosphorus. Phosphorus actively promotes dealumination during thermal treatment. The loss of Si–O–Al bonds and the expected reaction of phosphorus with Si–O–Al–OH species to form neutral local SAPO interfaces leads to permanent loss of Brønsted acid sites. Furthermore, the reversible interactions of phosphorus with framework aluminium before thermal treatment have been shown to lead to a loss of acid sites as well. At this moment, the exact nature of this reversible loss of acid sites is not understood. The choice of phosphorus precursor does not have a strong influence on the final effects of modification after thermal treatment, as phosphorus precursors decompose into (poly)phosphate species.

Besides a reduction in the number of acid sites, phosphatation also reduces the average strength of acid sites. An increase in phosphorus content leads to a further decrease in the average strength of acid sites. There are three causes for the observed decrease in average site strength. (i) A decrease in the acid site strength of bridging hydroxyl groups. (ii) Relatively more strong acid sites are removed by phosphatation than weak acid sites. (iii) An actual increase in the number of weak acid sites. Possible candidates for these new weak acid sites are silanol nests, extra-framework aluminium species and P–OH groups. The question of how the average acid site strength is reduced and what the source of new weak acid sites is demands more detailed and systematic characterisation studies.

Phosphorus has been shown to have a promotional effect on the hydrothermal stability of zeolites H-ZSM-5 and H-IM-5. Relatively more strong acid sites are retained during hydrothermal treatment and the amount of tetrahedrally coordinated framework aluminium (TFAl) species that are expelled from the framework is either relatively or absolutely less than in unmodified samples. Like silicoaluminophosphates, local SAPO interfaces have been found to remain unaffected during steam treatment and, as aluminium remains fixed in the framework, the pore structure is better retained. With prolonged steam treatment all Si–O–Al bonds at the SAPO interfaces are hydrolysed, leading to the formation of extra-framework $AlPO_4$. Therefore, we suggest that SAPO interfaces form metastable intermediates during dealumination in the zeolite H-ZSM-5 and H-IM-5

channel systems. It is not at all certain if phosphorus has a similar promotional effect on other framework topologies, which should receive more emphasis in further research.

All these physicochemical effects change the activity and selectivity of phosphated zeolites in a range of catalytic applications. In the selective catalytic reduction of NO_x with ammonia over transition metal-exchanged zeolites, the presence of phosphorus is extremely damaging. The breaking of Si–O–Al bonds, leading to a reduction in framework negative charge and acid sites, leads to a decrease in chemisorbed NH_3 and NO_x species. In addition, the subsequent formation of metal oxides and phosphate species reduces the accessibility of the zeolites even more, leading to severe deactivation.

In catalytic processes to produce hydrocarbons, zeolites modified by phosphorus have generally higher selectivity towards light olefins, especially propylene, and retain higher activities with time on-stream compared to their non-phosphated counterparts, due to reduced formation of coke and improved hydrothermal stability. The decrease in the number of strong Brønsted acid sites and the increase in weak Brønsted acid sites or the weak/strong acid site ratio have most often been attributed as the origin of most changes in performance in catalytic reactions such as hydrocarbon cracking, methanol-to-olefins, dehydration of ethanol and alkylation of aromatics. Reactions that demand strong acid sites achieve reduced conversion with an increase in the phosphorus content. Often, applying higher reaction temperatures increases the overall catalytic conversion. The decrease in acid site number and average acid site strength leads to a reduction in secondary reactions, such as hydride transfer, cracking and cyclisation reactions. This prevents oligomerization of light olefins and formation of coke, as well as the cracking of products.

Besides chemical alterations, the introduction of phosphorus into the zeolite channel leads to decreased pore dimensions and reduced accessibility, which in turn lead to longer diffusion pathways for reactants and products. Therefore, products that diffuse rapidly out of the zeolite will be formed with improved selectivity. Phosphate species that are present in the pores act as steric impediments and hinder the formation of bulky (intermediate) products such as carbenium ions. Therefore, it is suggested that modification by phosphorus of H-ZSM-5 inhibits the bimolecular cracking mechanism in alkane cracking and the aromatic-based cycle in methanol-to-hydrocarbon reactions.

As post-modification of zeolites with phosphorus is a relatively inexpensive way to boost catalyst lifetime and selectivity towards light olefins, and especially as zeolites are important potential agents in future sustainable hydrocarbon production processes, it is of great importance to obtain a more fundamental understanding of the underlying physicochemical effects of phosphorus–zeolite chemistry. The universal concepts on phosphorus–zeolite chemistry that are presented in this review article help the aim to modify zeolites by phosphorus more rationally and can act as a frame of reference in future studies to fundamentally understand the interaction of zeolites with group VA elements in general.

Notes and references

1 U. Olsbye, S. Svelle, M. Bjørgen, P. Beato, T. V. W. Janssens, F. Joensen, S. Bordiga and K. P. Lillerud, *Angew. Chem., Int. Ed.*, 2012, **51**, 5810–5831.
2 G. W. Huber, S. Iborra and A. Corma, *Chem. Rev.*, 2006, **106**, 4044–4098.
3 M. Guisnet and J.-P. Gilson, *Zeolites for cleaner technologies*, Imperial College Press, London, 2002.
4 S. Brandenberger, O. Kröcher, A. Tissler and R. Althoff, *Catal. Rev.*, 2008, **50**, 492–531.
5 L. Karwacki, M. H. F. Kox, D. A. Matthijs de Winter, M. R. Drury, J. D. Meeldijk, E. Stavitski, W. Schmidt, M. Mertens, P. Cubillas, N. John, A. Chan, N. Kahn, S. R. Bare, M. Anderson, J. Kornatowski and B. M. Weckhuysen, *Nat. Mater.*, 2009, **8**, 959–965.
6 G. Reding, T. Mäurer and B. Kraushaar-Czarnetzki, *Microporous Mesoporous Mater.*, 2003, **57**, 83–92.
7 Y. Yan, M. E. Davis and G. R. Gavalas, *Ind. Eng. Chem. Res.*, 1995, **34**, 1652–1661.
8 D. H. Olson, G. T. Kokotailo, S. L. Lawton and W. M. Meier, *J. Phys. Chem.*, 1981, **85**, 2238–2243.
9 www.iza-structure.org.
10 N. Y. Chen, W. W. Kaeding and F. G. Dwyer, *J. Am. Chem. Soc.*, 1979, **101**, 6783–6784.
11 Z. Y. Zakaria, N. A. S. Amin and J. Linnekoski, *Biomass Bioenergy*, 2013, **55**, 370–385.
12 J. Jae, R. Coolman, T. J. Mountziaris and G. W. Huber, *Chem. Eng. Sci.*, 2014, **108**, 33–46.
13 M. Takeuchi, T. Kimura, M. Hidaka, D. Rakhmawaty and M. Anpo, *J. Catal.*, 2007, **246**, 235–240.
14 R. K. Grasselli, D. L. Stern and J. G. Tsikoyiannis, *Appl. Catal., A*, 1999, **189**, 1–8.
15 W. O. Haag, R. M. Lago and P. G. Rodewald, *J. Mol. Catal.*, 1982, **17**, 161–169.
16 L. B. Young, S. A. Butter and W. W. Kaeding, *J. Catal.*, 1982, **76**, 418–432.
17 W. W. Kaeding, C. Chu, L. B. Young, B. Weinstein and S. A. Butter, *J. Catal.*, 1981, **67**, 159–174.
18 C. D. Chang and A. J. Silvestri, *J. Catal.*, 1977, **47**, 249–259.
19 W. R. Moser, R. W. Thompson, C.-C. Chiang and H. Tong, *J. Catal.*, 1989, **117**, 19–32.
20 T. F. Degnan, C. M. Smith and C. R. Venkat, *Appl. Catal., A*, 2001, **221**, 283–294.
21 K. Tanabe and W. F. Hölderich, *Appl. Catal., A*, 1999, **181**, 399–434.
22 H. Mooiweer, K. De Jong, B. Kraushaar-Czarnetzki, W. Stork and B. Krutzen, *Stud. Surf. Sci. Catal.*, 1994, **84**, 2327–2334.
23 G. Cao, L. R. M. Martens, J. L. White, T. J. Chen and M. J. Shah, US6080303 A, 2000.
24 C. Plank, E. Rosinski and W. Hawthorne, *Ind. Eng. Chem. Prod. Res. Dev.*, 1964, **3**, 165–169.
25 J. E. Otterstedt, S. B. Gevert, S. G. Jääs and P. G. Menon, *Appl. Catal.*, 1986, **22**, 159–179.
26 J. W. Ward, *Fuel Process. Technol.*, 1993, **35**, 55–85.

27 T. F. Degnan, G. K. Chitnis and P. H. Schipper, *Microporous Mesoporous Mater.*, 2000, **35–36**, 245–252.
28 A. Corma, V. Fornes, W. Kolodziejski and L. J. Martinez-Triguero, *J. Catal.*, 1994, **145**, 27–36.
29 J. C. Védrine, A. Auroux, P. Dejaifve, V. Ducarme, H. Hoser and S. Zhou, *J. Catal.*, 1982, **73**, 147–160.
30 A. F. Costa, H. S. Cerqueira, J. M. M. Ferreira, N. M. S. Ruiz and S. M. C. Menezes, *Appl. Catal., A*, 2007, **319**, 137–143.
31 J. Liu, C. Zhang, Z. Shen, W. Hua, Y. Tang, W. Shen, Y. Yue and H. Xu, *Catal. Commun.*, 2009, **10**, 1506–1509.
32 R. Silver, M. Stefanick and B. Todd, *Catal. Today*, 2008, **136**, 28–33.
33 G. Caeiro, P. Magnoux, J. M. Lopes, F. R. Ribeiro, S. M. C. Menezes, A. F. Costa and H. S. Cerqueira, *Appl. Catal., A*, 2006, **314**, 160–171.
34 T. Blasco, A. Corma and J. Martínez-Triguero, *J. Catal.*, 2006, **237**, 267–277.
35 J. A. Lercher and G. Rumplmayr, *Appl. Catal.*, 1986, **25**, 215–222.
36 H. L. Janardhan, G. V. Shanbhag and A. B. Halgeri, *Appl. Catal., A*, 2014, **471**, 12–18.
37 I. Lezcano-Gonzalez, U. Deka, H. E. van der Bij, P. Paalanen, B. Arstad, B. M. Weckhuysen and A. M. Beale, *Appl. Catal., B*, 2014, **154**, 339–349.
38 A. K. Ghosh, N. Kulkarni and P. L. Harvey, WO2014025371 A1, 2014.
39 D. H. Harris, WO2014042641 A1, 2014.
40 S. Mignard, A. Corma, J. Martinez-Triguero, E. Benazzi, S. Lacombe and G. Mabilon, US6306286 B1, 2001.
41 W. F. Lai, M. A. Hamilton and S. J. Mccarthy, WO2013059176 A1, 2013.
42 M. S. Al-Ghrami and C. Ercan, WO2013177388 A1, 2013.
43 G. Burghels, E. Corresa Mateu, S. Klingelhofer, J. Martinez-Triguero, M. Frauenrath and A. Corma, WO2012123558 A1, 2012.
44 L. A. Chewter, W. J. Van and F. Winter, WO2010133643 A2, 2010.
45 D. L. Johnson, K. E. Nariman and R. A. Ware, WO2001004237 A2, 2001.
46 A. Corma, WO1999002260 A1, 1999.
47 T. G. Roberie and F. T. I. I. John, US5286369 A, 1994.
48 G. W. Kirker, M. E. Landis and J. H. Yen, US4724066 A, 1988.
49 A. J. Tissler and E. T. C. Vogt, WO2001037994 A3, 2001.
50 G. Lischke, R. Eckelt, H. G. Jerschkewitz, B. Parlitz, E. Schreier, W. Storek, B. Zibrowius and G. Öhlmann, *J. Catal.*, 1991, **132**, 229–243.
51 M. J. B. Cardoso, D. D. O. Rosas and L. Y. Lau, *Adsorption*, 2005, **11**, 577–580.
52 W. W. Kaeding and S. A. Butter, *J. Catal.*, 1980, **61**, 155–164.
53 M. Göhlich, W. Reschetilowski and S. Paasch, *Microporous Mesoporous Mater.*, 2011, **142**, 178–183.
54 A. Jentys, G. Rumplmayr and J. A. Lercher, *Appl. Catal.*, 1989, **53**, 299–312.
55 K. Damodaran, J. W. Wiench, S. M. Cabral de Menezes, Y. L. Lam, J. Trebosc, J. P. Amoureux and M. Pruski, *Microporous Mesoporous Mater.*, 2006, **95**, 296–305.
56 J. Caro, M. Bülow, M. Derewinski, J. Haber, M. Hunger, J. Kärger, H. Pfeifer, W. Storek and B. Zibrowius, *J. Catal.*, 1990, **124**, 367–375.
57 N. Xue, X. Chen, L. Nie, X. Guo, W. Ding, Y. Chen, M. Gu and Z. Xie, *J. Catal.*, 2007, **248**, 20–28.
58 J. Zhuang, D. Ma, G. Yang, Z. Yan, X. Liu, X. Liu, X. Han, X. Bao, P. Xie and Z. Liu, *J. Catal.*, 2004, **228**, 234–242.
59 S. M. Abubakar, D. M. Marcus, J. C. Lee, J. O. Ehresmann, C. Y. Chen, P. W. Kletnieks, D. R. Guenther, M. J. Hayman, M. Pavlova, J. B. Nicholas and J. F. Haw, *Langmuir*, 2006, **22**, 4846–4852.
60 A. Yamaguchi, D. Jin, T. Ikeda, K. Sato, N. Hiyoshi, T. Hanaoka, F. Mizukami and M. Shirai, *Catal. Lett.*, 2014, **144**, 44–49.
61 S. M. Campbell, D. M. Bibby, J. M. Coddington and R. F. Howe, *J. Catal.*, 1996, **161**, 350–358.
62 A. T. Aguayo, A. G. Gayubo, A. M. Tarrío, A. Atutxa and J. Bilbao, *J. Chem. Technol. Biotechnol.*, 2002, **77**, 211–216.
63 Z. Song, A. Takahashi, I. Nakamura and T. Fujitani, *Appl. Catal., A*, 2010, **384**, 201–205.
64 G. Zhao, J. Teng, Z. Xie, W. Jin, W. Yang, Q. Chen and Y. Tang, *J. Catal.*, 2007, **248**, 29–37.
65 S. Shwan, J. Jansson, L. Olsson and M. Skoglundh, *Appl. Catal., B*, 2014, **147**, 111–123.
66 L. Lin, C. Qiu, Z. Zhuo, D. Zhang, S. Zhao, H. Wu, Y. Liu and M. He, *J. Catal.*, 2014, **309**, 136–145.
67 M. Derewinski, P. Sarv, X. Sun, S. Müller, A. C. Van Veen and J. A. Lercher, *J. Phys. Chem. C*, 2014, **118**, 6122–6131.
68 K. H. Chandawar, S. B. Kulkarni and P. Ratnasamy, *Appl. Catal.*, 1982, **4**, 287–295.
69 G. Seo and R. Ryoo, *J. Catal.*, 1990, **124**, 224–230.
70 V. N. Romannikov, A. J. Tissler and R. Thome, *React. Kinet. Catal. Lett.*, 1993, **51**, 125–134.
71 S. M. Cabral de Menezes, Y. L. Lam, K. Damodaran and M. Pruski, *Microporous Mesoporous Mater.*, 2006, **95**, 286–295.
72 M. Ghiaci, A. Abbaspur, M. Arshadi and B. Aghabarari, *Appl. Catal., A*, 2007, **316**, 32–46.
73 M. Ghiaci, A. Abbaspur and R. J. Kalbasi, *Appl. Catal., A*, 2006, **298**, 32–39.
74 R. J. Kalbasi, M. Ghiaci and A. R. Massah, *Appl. Catal., A*, 2009, **353**, 1–8.
75 R. Lü, Z. Cao and X. Liu, *J. Nat. Gas Chem.*, 2008, **17**, 142–148.
76 G. Jiang, L. Zhang, Z. Zhao, X. Zhou, A. Duan, C. Xu and J. Gao, *Appl. Catal., A*, 2008, **340**, 176–182.
77 D. Zhang, R. Wang and X. Yang, *Catal. Lett.*, 2008, **124**, 384–391.
78 Y.-J. Lee, J. M. Kim, J. W. Bae, C.-H. Shin and K.-W. Jun, *Fuel*, 2009, **88**, 1915–1921.
79 N. Xue, L. Nie, D. Fang, X. Guo, J. Shen, W. Ding and Y. Chen, *Appl. Catal., A*, 2009, **352**, 87–94.
80 Z. Wang, G. Jiang, Z. Zhao, X. Feng, A. Duan, J. Liu, C. Xu and J. Gao, *Energy Fuels*, 2009, **24**, 758–763.
81 K. Ramesh, L. M. Hui, Y.-F. Han and A. Borgna, *Catal. Commun.*, 2009, **10**, 567–571.
82 P. Li, W. Zhang, X. Han and X. Bao, *Catal. Lett.*, 2010, **134**, 124–130.

83 N. Zhan, Y. Hu, H. Li, D. Yu, Y. Han and H. Huang, *Catal. Commun.*, 2010, **11**, 633–637.
84 K. Ramesh, C. Jie, Y.-F. Han and A. Borgna, *Ind. Eng. Chem. Res.*, 2011, **49**, 4080–4090.
85 D. Liu, W. C. Choi, C. W. Lee, N. Y. Kang, Y. J. Lee, C.-H. Shin and Y. K. Park, *Catal. Today*, 2011, **164**, 154–157.
86 H. E. van der Bij and B. M. Weckhuysen, *Phys. Chem. Chem. Phys.*, 2014, **16**, 9892–9903.
87 H. E. van der Bij, L. R. Aramburo, B. Arstad, J. J. Dynes, J. Wang and B. M. Weckhuysen, *ChemPhysChem*, 2014, **15**, 283–292.
88 A. Corma, J. Mengual and P. J. Miguel, *Appl. Catal., A*, 2012, **421**, 121–134.
89 M. Dyballa, E. Klemm, J. Weitkamp and M. Hunger, *Chem. Eng. Technol.*, 2013, **85**, 1719–1725.
90 H. Vinek, G. Rumplmayr and J. A. Lercher, *J. Catal.*, 1989, **115**, 291–300.
91 G. Rumplmayr and J. A. Lercher, *Zeolites*, 1990, **10**, 283–287.
92 N. Xue, R. Olindo and J. A. Lercher, *J. Phys. Chem. C*, 2010, **114**, 15763–15770.
93 W. W. Kaeding, C. Chu, L. B. Young and S. A. Butter, *J. Catal.*, 1981, **69**, 392–398.
94 P. Tynjälä, T. T. Pakkanen and S. Mustamaki, *J. Phys. Chem. B*, 1998, **102**, 5280–5286.
95 J. Nunan, J. Cronin and J. Cunningham, *J. Catal.*, 1984, **87**, 77–85.
96 A. Rahman, G. Lemay, A. Adnot and S. Kaliaguine, *J. Catal.*, 1988, **112**, 453–463.
97 A. Rahman, A. Adnot, G. Lemay, S. Kaliaguine and G. Jean, *Appl. Catal.*, 1989, **50**, 131–147.
98 M. Kojima, F. Lefebvre and Y. Ben Taârit, *Zeolites*, 1992, **12**, 724–727.
99 W. Reschetilowski, B. Meier, M. Hunger, B. Unger and K. P. Wendlandt, *Angew. Chem., Int. Ed.*, 1991, **30**, 686–687.
100 B. Viswanathan and A. C. Pulikottil, *Catal. Lett.*, 1993, **22**, 373–379.
101 X. Gao, Z. Tang, D. Ji and H. Zhang, *Catal. Commun.*, 2009, **10**, 1787–1790.
102 X. Gao, Z. Tang, H. Zhang, C. Liu, Z. Zhang, G. Lu and D. Ji, *Korean J. Chem. Eng.*, 2010, **27**, 812–815.
103 Y. Huang, X. Dong, M. Li, M. Zhang and Y. Yu, *RSC Adv.*, 2014, **4**, 14573–14581.
104 T. Fjermestad, S. Svelle and O. Swang, *J. Phys. Chem. C*, 2013, **117**, 13442–13451.
105 S. Malola, S. Svelle, F. L. Bleken and O. Swang, *Angew. Chem., Int. Ed.*, 2012, **51**, 652–655.
106 S. M. Campbell, D. M. Bibby, J. M. Coddington, R. F. Howe and R. H. Meinhold, *J. Catal.*, 1996, **161**, 338–349.
107 H. E. van der Bij, F. Meirer, S. Kalirai, J. Wang and B. M. Weckhuysen, *Chem. – Eur. J.*, 2014, **20**, 16922–16932.
108 S. M. Bradley and R. F. Howe, *Microporous Mater.*, 1997, **12**, 13–19.
109 Z. Liu, Z.-X. Chen, W. Ding, G.-J. Kang and Z. Li, *THEOCHEM*, 2010, **948**, 99–101.
110 P. H. Zeng, Y. Liang, S. F. Ji, B. J. Shen, H. H. Liu, B. J. Wang, H. J. Zhao and M. F. Li, *J. Energy Chem.*, 2014, **23**, 193–200.
111 M. Hunger, *Zeolites and Catalysis: Synthesis, Reactions and Applications*, Wiley-VCH, Weinheim, 2010, vol. 2, pp. 493–546.
112 X. Wang, W. Dai, G. Wu, L. Li, N. Guan and M. Hunger, *Microporous Mesoporous Mater.*, 2012, **151**, 99–106.
113 H. E. Van der Bij, D. Cicmil, J. Wang, F. Meirer, F. M. F. de Groot and B. M. Weckhuysen, *J. Am. Chem. Soc.*, 2014, **136**, 17774–17787.
114 E. W. Shin, J. S. Han, M. Jang, S.-H. Min, J. K. Park and R. M. Rowell, *Environ. Sci. Technol.*, 2003, **38**, 912–917.
115 J. W. Wiench, G. Tricot, L. Delevoye, J. Trebosc, J. Frye, L. Montagne, J.-P. Amoureux and M. Pruski, *Phys. Chem. Chem. Phys.*, 2006, **8**, 144–150.
116 Y. Wang, B. Shen, L. Wang, B. Feng, J. Li and Q. Guo, *Fuel Process. Technol.*, 2013, **106**, 141–148.
117 M. Müller, G. Harvey and R. Prins, *Microporous Mesoporous Mater.*, 2000, **34**, 135–147.
118 G. Sastre, D. W. Lewis and C. R. A. Catlow, *J. Phys. Chem.*, 1996, **100**, 6722–6730.
119 D. Barthomeuf, *Zeolites*, 1994, **14**, 394–401.
120 J. Tan, Z. Liu, X. Bao, X. Liu, X. Han, C. He and R. Zhai, *Microporous Mesoporous Mater.*, 2002, **53**, 97–108.
121 S. L. Suib, A. M. Winiecki and A. Kostapapas, *Langmuir*, 1987, **3**, 483–488.
122 R. Lü, Z. Cao and S. Wang, *THEOCHEM*, 2008, **865**, 1–7.
123 R. M. Barrer and M. Liquornik, *J. Chem. Soc., Dalton Trans.*, 1974, 2126–2128.
124 N. J. Clayden, S. Esposito, P. Pernice and A. Aronne, *J. Mater. Chem.*, 2001, **11**, 936–943.
125 C. Coelho, T. Azaïs, L. Bonhomme-Coury, G. Laurent and C. Bonhomme, *Inorg. Chem.*, 2007, **46**, 1379–1387.
126 G. H. Kühl and K. D. Schmitt, *Zeolites*, 1990, **10**, 2–7.
127 A. Corma, J. Mengual and P. J. Miguel, *Appl. Catal., A*, 2013, **460–461**, 106–115.
128 Q. Cui, Y. Zhou, Q. Wei, G. Yu and L. Zhu, *Fuel Process. Technol.*, 2013, **106**, 439–446.
129 Y. Wang, B. Shen, K. Hao, J. Li, L. Wang, B. Feng and Q. Guo, *Catal. Commun.*, 2012, **25**, 59–63.
130 E. Loeffler, U. Lohse, C. Peuker, G. Oehlmann, L. M. Kustov, V. L. Zholobenko and V. B. Kazansky, *Zeolites*, 1990, **10**, 266–271.
131 J. A. van Bokhoven, A. M. J. van der Eerden and D. C. Koningsberger, *J. Am. Chem. Soc.*, 2003, **125**, 7435–7442.
132 B. Zhao, H. Pan and J. H. Lunsford, *Langmuir*, 1999, **15**, 2761–2765.
133 C. Liu, X. Gao, Z. Zhang, H. Zhang, S. Sun and Y. Deng, *Appl. Catal., A*, 2004, **264**, 225–228.
134 P. Tynjälä and T. T. Pakkanen, *Microporous Mesoporous Mater.*, 1998, **20**, 363–369.
135 J. Gopalakrishnan, *Chem. Mater.*, 1995, **7**, 1265–1275.
136 S. van Donk, A. H. Janssen, J. H. Bitter and K. P. de Jong, *Catal. Rev.*, 2003, **45**, 297–319.
137 M.-C. Silaghi, C. Chizallet and P. Raybaud, *Microporous Mesoporous Mater.*, 2014, **191**, 82–96.
138 O. Lisboa, M. Sánchez and F. Ruette, *J. Mol. Catal. A: Chem.*, 2008, **294**, 93–101.

139 T. Chevreau, A. Chambellan, J. Lavalley, E. Catherine, M. Marzin, A. Janin, J. Hemidy and S. Khabtou, *Zeolites*, 1990, **10**, 226–234.
140 C. S. Triantafillidis, A. G. Vlessidis, L. Nalbandian and N. P. Evmiridis, *Microporous Mesoporous Mater.*, 2001, **47**, 369–388.
141 T.-H. Chen, K. Houthoofd and P. J. Grobet, *Microporous Mesoporous Mater.*, 2005, **86**, 31–37.
142 J. Jiao, J. Kanellopoulos, W. Wang, S. S. Ray, H. Foerster, D. Freude and M. Hunger, *Phys. Chem. Chem. Phys.*, 2005, **7**, 3221–3226.
143 Z. Yu, S. Li, Q. Wang, A. Zheng, X. Jun, L. Chen and F. Deng, *J. Phys. Chem. C*, 2011, **115**, 22320–22327.
144 I. Wang, T.-J. Chen, K.-J. Chao and T.-C. Tsai, *J. Catal.*, 1979, **60**, 140–147.
145 L. R. Aramburo, E. de Smit, B. Arstad, M. M. van Schooneveld, L. Sommer, A. Juhin, T. Yokosawa, H. W. Zandbergen, U. Olsbye, F. M. F. de Groot and B. M. Weckhuysen, *Angew. Chem., Int. Ed.*, 2012, **51**, 3616–3619.
146 S. M. T. Almutairi, B. Mezari, E. A. Pidko, P. C. M. M. Magusin and E. J. M. Hensen, *J. Catal.*, 2013, **307**, 194–203.
147 A. Corma, M. Faraldos and A. Mifsud, *Appl. Catal.*, 1989, **47**, 125–133.
148 G. T. Kerr, *J. Phys. Chem.*, 1967, **71**, 4155–4156.
149 C. S. Cundy and P. A. Cox, *Chem. Rev.*, 2003, **103**, 663–702.
150 R. Ryoo and S. Jun, *J. Phys. Chem. B*, 1997, **101**, 317–320.
151 L. R. Aramburo, Y. Liu, T. Tyliszczak, F. M. F. de Groot, J. C. Andrews and B. M. Weckhuysen, *ChemPhysChem*, 2013, **14**, 496–499.
152 L. R. Aramburo, L. Karwacki, P. Cubillas, S. Asahina, D. A. M. de Winter, M. R. Drury, I. L. C. Buurmans, E. Stavitski, D. Mores, M. Daturi, P. Bazin, P. Dumas, F. Thibault-Starzyk, J. A. Post, M. W. Anderson, O. Terasaki and B. M. Weckhuysen, *Chem. – Eur. J.*, 2011, **17**, 13773–13781.
153 J. Jiao, S. Altwasser, W. Wang, J. Weitkamp and M. Hunger, *J. Phys. Chem. B*, 2004, **108**, 14305–14310.
154 M. Briend, A. Shikholeslami, M.-J. Peltre, D. Delafosse and D. Barthomeuf, *J. Chem. Soc., Dalton Trans.*, 1989, 1361–1362.
155 S. Wilson and P. Barger, *Microporous Mesoporous Mater.*, 1999, **29**, 117–126.
156 J. P. Loureno, M. F. Ribeiro, F. R. Ribeiro, J. Rocha, Z. Gabelica and E. G. Derouane, *Microporous Mater.*, 1995, **4**, 445–453.
157 L. Huang and Q. Li, *Chem. Lett.*, 1999, 829–830.
158 M. Bjørgen, F. Joensen, M. Spangsberg Holm, U. Olsbye, K.-P. Lillerud and S. Svelle, *Appl. Catal., A*, 2008, **345**, 43–50.
159 U. Deka, I. Lezcano-Gonzalez, B. M. Weckhuysen and A. M. Beale, *ACS Catal.*, 2013, **3**, 413–427.
160 M. Devadas, O. Kröcher, M. Elsener, A. Wokaun, G. Mitrikas, N. Söger, M. Pfeifer, Y. Demel and L. Mussmann, *Catal. Today*, 2007, **119**, 137–144.
161 P. Kern, M. Klimczak, T. Heinzelmann, M. Lucas and P. Claus, *Appl. Catal., B*, 2010, **95**, 48–56.
162 S. Kotrel, H. Knözinger and B. C. Gates, *Microporous Mesoporous Mater.*, 2000, **35–36**, 11–20.
163 A. Corma and A. V. Orchillés, *Microporous Mesoporous Mater.*, 2000, **35–36**, 21–30.
164 C. B. Phillips and R. Datta, *Ind. Eng. Chem. Res.*, 1997, **36**, 4466–4475.
165 W. Dai, X. Wang, G. Wu, L. Li, N. Guan and M. Hunger, *ChemCatChem*, 2012, **4**, 1428–1435.
166 C. D. Chang, C. T. W. Chu and R. F. Socha, *J. Catal.*, 1984, **86**, 289–296.
167 C. Mei, P. Wen, Z. Liu, H. Liu, Y. Wang, W. Yang, Z. Xie, W. Hua and Z. Gao, *J. Catal.*, 2008, **258**, 243–249.
168 F. L. Bleken, S. Chavan, U. Olsbye, M. Boltz, F. Ocampo and B. Louis, *Appl. Catal., A*, 2012, **447–448**, 178–185.
169 A. F. H. Wielers, M. Vaarkamp and M. F. M. Post, *J. Catal.*, 1991, **127**, 51–66.
170 B. S. Greensfelder, H. H. Voge and G. M. Good, *Ind. Eng. Chem.*, 1949, **41**, 2573–2584.
171 N. Rahimi and R. Karimzadeh, *Appl. Catal., A*, 2011, **398**, 1–17.
172 F. C. Jentoft and B. C. Gates, *Top. Catal.*, 1997, **4**, 1–13.
173 K. Kubo, H. Iida, S. Namba and A. Igarashi, *Microporous Mesoporous Mater.*, 2014, **188**, 23–29.
174 F. Bleken, M. Bjørgen, L. Palumbo, S. Bordiga, S. Svelle, K.-P. Lillerud and U. Olsbye, *Top. Catal.*, 2009, **52**, 218–228.
175 A. Takahashi, W. Xia, I. Nakamura, H. Shimada and T. Fujitani, *Appl. Catal., A*, 2012, **423**, 162–167.
176 S. Teketel, S. Svelle, K.-P. Lillerud and U. Olsbye, *ChemCatChem*, 2009, **1**, 78–81.
177 F. Bager, N. L. Salas and S. Ernst, *Oil Gas Eur. Mag.*, 2012, **38**, 107–111.
178 R. Bastiani, Y. L. Lam, C. A. Henriques and V. Teixeira da Silva, *Fuel*, 2013, **107**, 680–687.
179 O. Bortnovsky, P. Sazama and B. Wichterlova, *Appl. Catal., A*, 2005, **287**, 203–213.
180 D. Mores, E. Stavitski, M. H. F. Kox, J. Kornatowski, U. Olsbye and B. M. Weckhuysen, *Chem. – Eur. J.*, 2008, **14**, 11320–11327.
181 M. J. Wulfers and F. C. Jentoft, *J. Catal.*, 2013, **307**, 204–213.
182 Y. Furumoto, Y. Harada, N. Tsunoji, A. Takahashi, T. Fujitani, Y. Ide, M. Sadakane and T. Sano, *Appl. Catal., A*, 2011, **399**, 262–267.
183 Y.-J. Lee, Y.-W. Kim, N. Viswanadham, K.-W. Jun and J. W. Bae, *Appl. Catal., A*, 2010, **374**, 18–25.
184 G. Majano, L. Delmotte, V. Valtchev and S. Mintova, *Chem. Mater.*, 2009, **21**, 4184–4191.
185 F. J. Machado, C. M. López, M. a. A. Centeno and C. Urbina, *Appl. Catal., A*, 1999, **181**, 29–38.
186 M. Hartmann, *Angew. Chem., Int. Ed.*, 2004, **43**, 5880–5882.
187 J. Perez-Ramirez, C. H. Christensen, K. Egeblad, C. H. Christensen and J. C. Groen, *Chem. Soc. Rev.*, 2008, **37**, 2530–2542.
188 Y. Xu, T. Nakajima and A. Ohki, *J. Hazard. Mater.*, 2002, **92**, 275–287.
189 S. Shevade and R. G. Ford, *Water Res.*, 2004, **38**, 3197–3204.
190 P. Chutia, S. Kato, T. Kojima and S. Satokawa, *J. Hazard. Mater.*, 2009, **162**, 440–447.
191 D. Mao, J. Xia, B. Zhang and G. Lu, *Energy Convers. Manage.*, 2010, **51**, 1134–1139.
192 S. Zheng, A. Jentys and J. A. Lercher, *J. Catal.*, 2003, **219**, 310–319.

